



iMScope QT

Imaging Mass Microscope

Unrivaled Mass Spectrometry Imaging Platform

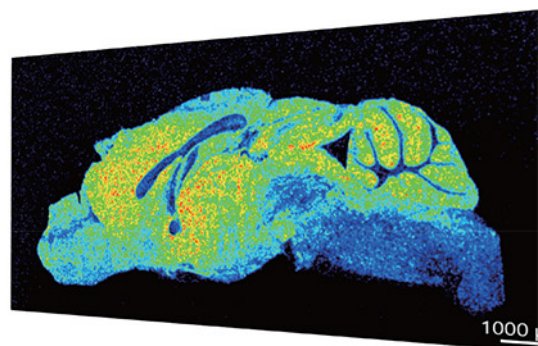
With unparalleled speed, sensitivity and spatial resolution, Shimadzu's **iMScope QT imaging mass microscope** clears the way to next-generation mass spectrometry imaging.

- Fast acquisition of high-mass, high-resolution images at the optical and molecular level
- Simultaneously visualize and analyze samples
- Full fusion with morphology studies
- Integration with the Q-TOF LCMS-9030 enables obtaining distribution information and quantitative data for comprehensive analysis
- Easy switching between MS imaging configuration and LCMS

Learn more about Shimadzu's iMScope QT.

Visit us online at www.ssi.shimadzu.com

Shimadzu Scientific Instruments Inc., 7102 Riverwood Dr., Columbia, MD 21046, USA



The potential of NO^+ and $\text{O}_2^{+\bullet}$ in switchable reagent ion proton transfer reaction time-of-flight mass spectrometry

Oliver Hegen¹ | Jorge I. Salazar Gómez¹  | Robert Schlögl^{1,2}  | Holger Ruland¹ 

¹Department of Heterogeneous Reactions, Max Planck Institute for Chemical Energy Conversion, Mülheim an der Ruhr, Deutschland

²Department of Inorganic Chemistry, Fritz Haber Institute of the Max Planck Society, Berlin, Germany

Correspondence

Oliver Hegen and Holger Ruland Max Planck Institute for Chemical Energy Conversion, Stiftstraße 34–36, 45470 Mülheim an der Ruhr, Germany.
Email: oliver-niklas.hegen@cec.mpg.de and holger.ruland@cec.mpg.de

Abstract

Selected ion flow tube mass spectrometry (SIFT-MS) and proton transfer reaction mass spectrometry with switchable reagent ion capability (PTR+SRI-MS) are analytical techniques for real-time qualification and quantification of compounds in gas samples with trace level concentrations. In the detection process, neutral compounds—mainly volatile organic compounds—are ionized via chemical ionization with ionic reagents or primary ions. The most common reagent ions are H_3O^+ , NO^+ and $\text{O}_2^{+\bullet}$. While ionization with H_3O^+ occurs by means of proton transfer, the ionization via NO^+ and $\text{O}_2^{+\bullet}$ offers a larger variety on ionization pathways, as charge transfer, hydride abstraction and so on are possible. The distribution of the reactant into various reaction channels depends not only on the usage of either NO^+ or $\text{O}_2^{+\bullet}$, but also on the class of analyte compounds. Furthermore, the choice of the reaction conditions as well as the choice of either SIFT-MS or PTR+SRI-MS might have a large impact on the resulting products. Therefore, an overview of both NO^+ and $\text{O}_2^{+\bullet}$ as reagent ions is given, showing differences between SIFT-MS and PTR+SRI-MS as used analytical methods revealing the potential how the knowledge obtained with H_3O^+ for different classes of compounds can be extended with the usage of NO^+ and $\text{O}_2^{+\bullet}$.

KEYWORDS

NO^+ - $\text{O}_2^{+\bullet}$ - H_3O^+ -mass spectrometry, PTR-MS, SIFT-MS

1 | INTRODUCTION

The analysis of trace compounds, especially volatile organic compounds (VOCs), is a common, albeit challenging task in the field of gas analysis. For instance, an enormous variety of VOCs are present in air at ppmv, ppbv and even pptv levels. Some trace compounds exhibit a lifetime in earth's atmosphere of only a few minutes before being oxidized (Atkinson & Arey, 2003). Given these considerations, conventional approaches to

gas analysis, such as gas chromatography coupled with mass spectrometry (GC-MS), are not feasible for this kind of problem. In general, it is not feasible for such analysis to isolate and additionally calibrate individual components. For such situations alternative techniques like proton transfer reaction mass spectrometry (PTR-MS) are applied.

The technique of PTR-MS is a descendant of chemical ionization mass spectrometry (CI-MS) (Fehsenfeld et al., 1966). The selected ion flow tube (SIFT-) technique was

This is an open access article under the terms of the Creative Commons Attribution License, which permits use, distribution and reproduction in any medium, provided the original work is properly cited.

© 2022 The Authors. *Mass Spectrometry Reviews* published by John Wiley & Sons Ltd.

introduced in 1976 by N. G. Adams and Smith (1976) to study ion–molecule reaction kinetics, and improved several times while evolving into its current form (Smith & Španěl, 2005). After its coupling to a mass spectrometer, SIFT-MS made its first appearance as analytical technique for trace compounds in 1996 (Smith & Španěl, 1996). In that process, a selected ion, such as H_3O^+ , NO^+ or O_2^+ , reacts with the trace gases in the sample, allowing a qualitative and quantitative analysis in the ppbv range within seconds. The range of analytes was further extended by the work of Hera et al. in 2017, who introduced five anions, O^- , OH^- , O_2^- , NO_2^- and NO_3^- as reagent ions in SIFT-MS (Hera et al., 2017). In comparison, PTR-MS was introduced in its current form in 1995 (Hansel et al., 1995), but originated from selected ion flow-drift tube mass spectrometry (SIFDFT-MS), which combines SIFT with a flow-drift tube (Smith et al., 2014; Smith, Španěl, et al., 2014).

Both SIFT-MS and PTR-MS find numerous applications in several different research fields. Not only in atmospheric (de Gouw & Warneke, 2007; de Gouw, Goldan, et al. 2003; de Gouw, Warneke, et al., 2003; Lehnert et al., 2020; Smith, 1996; Yuan et al., 2017; Zhao, Zhang, Fortner, et al., 2004) and environmental research (Biasioli et al., 2011; de Gouw & Warneke, 2007; Hayward et al., 2002; Smith et al., 1998, 2002), but also in fields like biology (Smith & Španěl, 2011; Yuan et al., 2014), food and flavor science (Biasioli et al., 2011; Fabris et al., 2010; Gallardo-Escamilla et al., 2005; Sanchez del Pulgar et al., 2013; Yeretzian et al., 2003), agricultural science (Hastie et al., 2021), industry (Knighton et al., 2012) and medicine (Herbig et al., 2009; Jurschik et al., 2012; Lirk et al., 2004; Pugliese et al., 2019; Smith et al., 1999). The determination of trace gases is of high importance for the understanding of complex chemical processes.

In SIFT-MS, a series of positive ions are generated in an ion source, for example, by microwave discharge source. The positive ions are filtered a quadrupole mass filter, whereby a selected mass-to-charge-ratio is allowed to pass. After injection into a fast-flowing inert gas (e.g., He), which contains the analyte gas, the ions diffuse further along the flow tube as a cold ion swarm, and are thermalized (80–600K) (Smith & Adams, 1987). The ions are sampled via a pinhole orifice into a differentially pumped mass spectrometer, and subsequently detected with, for example, a channeltron or pulse counting system (Španěl & Smith, 1996a, 1996b). Further mechanistic details and insights into the underlying physics are given in the reviews of Smith and Španěl (2005) and Španěl and Smith (1996a). In addition, we would like to mention the review by Ard et al. (2021) which presents one of the most advanced contemporary versions of a SIFT, in terms

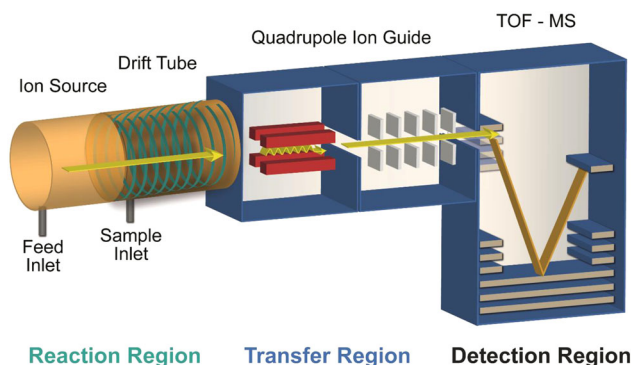


FIGURE 1 Schematic drawing of a proton-transfer-reaction time-of-flight mass spectrometer with quadrupole interface

of source improvement and detection capabilities, which is currently located at the Air Force Research Laboratory in the United States.

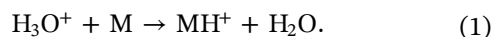
The development of PTR-MS (Figure 1), improved on two major difficulties of SIFT-MS with regard to the generation of H_3O^+ and NO^+ . First, by using a hollow-cathode discharge as an ion source, the generation of reagent ions takes place in a much higher efficiency in PTR-MS compared to SIFT-MS. This aspect makes the injection mass filter unnecessary. Second, the replacement of the diffusion-driven flow tube in SIFT-MS by an electrostatic-driven drift tube in PTR-MS, reduces the formation of clusters, like $(\text{H}_3\text{OM})^+$ and $(\text{NOM})^+$. Both improvements lead to a much higher detection sensitivity in PTR-MS, achieving sensitivities in pptv range (Graus et al., 2010; IONICON, 2019; White et al., 2013).

However, since its introduction by Hansel et al. (1995), several variations of PTR-MS device were developed, differing especially in terms of the ion separation, leading to various mass resolution and sensitivities. With regard to the measuring task, a high mass resolution, ideally over $5000\text{ m}/\Delta m$, is required to identify some isobaric VOCs, like protonated glyoxal ($\text{CH}(\text{O})\text{CH}(\text{O})\text{H}^+$) and protonated acetone ($\text{CH}_3\text{C}(\text{O})\text{CH}_3\text{H}^+$) (Graus et al., 2010). Furthermore, taking the analysis of complex analytes into account, a good signal-to-noise ratio (S/N) and, therefore, a high sensitivity is indispensable to obtain reliable results (de Gouw & Warneke, 2007; Pagonis et al., 2019; Yeretzian et al., 2003; Yuan et al., 2014). Besides the Ion Trap MS (Mielke et al., 2008; Prazeller et al., 2003; Warneke et al., 2005), which was a custom-built device, several versions of time-of-flight MS (TOF-MS, e.g., proton-transfer-reaction time-of-flight mass spectrometer with quadrupole interface in Figure 1) (Blake et al., 2004; 2009; Jordan et al., 2009b; Sulzer et al., 2014) and Quadrupole MS (Hansel et al., 1995; Jordan et al., 2009a; Lindinger et al., 1998) are commercially available. A detailed overview of the various

commercially available PTR-MS devices is given by Yuan et al. (2017).

Compared to other trace gas analysis techniques, for example, Electron ionization mass spectrometry (EI-MS), PTR-MS offers three major advantages. The analysis of VOCs in PTR-MS shows much less fragmentation compared to EI-MS, which is especially important for the analysis of complex samples. Generally, EI-MS analysis leads to an extremely complex spectra due to the fragmentation processes (Lindinger et al., 2005). Additionally, the application as a semi-quantitative method ($\pm 30\%$) gives PTR-MS the unique ability to quantify certain analytes without further calibration (IONICON, 2019), which is not generally possible with an EI-MS. Furthermore, in PTR-MS, low levels of analyte can be detected on-line without pre-concentration, which is often necessary in EI-MS (Maleknia et al., 2007).

The ionization method in PTR-MS, and also the most popular in SIFT-MS, occurs via a proton transfer reaction between H_3O^+ and an analyte molecule, leading to the nominal molecular mass +1 (Ellis & Mayhew, 2014). A successful proton transfer (Equation 1) depends not only on a higher proton affinity of the analyte compared to water (691 kJ mol^{-1}), but also on the collision rate.



The proton affinity of a given VOC indicates whether the reaction is thermodynamically favored. The collision rate constant k [$\text{cm}^3 \text{s}^{-1}$] is a purely kinetic factor that depends on the polarizability and the dipole moment of the molecule. Furthermore, while the k -rates are unique for every compound in a gas matrix, additionally they depend on the reduced electric field strength E/N [Td] in a PTR-MS. E/N is a ratio of the electric field to the gas density number N in the drift tube and determines the residence time and the kinetic energy of the ions in the drift tube (IONICON, 2019). It depends on the temperature as well as the pressure and the voltages inside the drift tube. Summarizing all this information, assuming $[\text{M}] \ll [\text{H}_3\text{O}^+]$, meaning the concentration of the reagent ion does not change significantly during the reaction, the concentration of $[\text{M}]$ in PTR-MS can be calculated via Equation (2):

$$[\text{M}] = \frac{[\text{AH}^+]}{[\text{H}_3\text{O}^+]} \times \frac{1}{k_{\text{tr}}}. \quad (2)$$

Besides the k -ratio, which if calculated (Strekowski et al., 2019) and experimentally (Zhao & Zhang, 2004) proven may have an error margin of up to 50% to the mean value, further approximations are made which might have a huge impact to the determination of a

certain compound concentration (Blake et al., 2009). The temperatures at which the ion-molecule collisions take place can be estimated, but it remains unclear if this temperature accurately reflects the ion chemistry inside the drift tube. Furthermore, the transit time of the ion across the drift tube, as well as, the ion transmission as a function of m/z also has some uncertainty. As shown by Keck et al. (2007) light inorganic ions, having nearly the same mass, have mobilities inside the drift tube that can differ by up to 20% (NO^+ : $3.2 \text{ cm}^2 \text{V}^{-1} \text{s}^{-1}$; O_2^+ : $2.6 \text{ cm}^2 \text{V}^{-1} \text{s}^{-1}$). This uncertainty can be expected to increase for heavier molecules. Another influential parameter, aside the properties of the determined component, is the device settings and the gas matrix, especially the humidity of the gas sample (de Gouw & Warneke, 2007). It is highly desirable to choose an E/N value that is high enough to prevent cluster development of the analytes with the reagent ion as well as with water molecules, and low enough to result in as little fragmentation as possible. However, in highly humid gas samples, water clustering cannot be avoided, making the choice of the E/N value always a compromise. Furthermore, fragmentation cannot be ruled out for certain analytes (Misztal et al., 2012). As a result, a certain signal can be generated through the molecular ion or a fragment of a heavier molecule or both, making a quantification in a complex gas sample a highly demanding task.

Taking all these approximations and uncertainties into account, PTR-MS can be seen as a semiquantitative method giving at least the range of the concentration of a certain compound in a complex gas sample. However, applying a suitable calibration for certain analytes a quantification with an error margin of 10-25% is accessible (Blake et al., 2009).

The reagent ion H_3O^+ is formed by a multistep reaction in the ion source. First, the prereagent ions H_2O^+ , OH^+ , O^+ , H_2^+ and H^+ are formed via a hollow cathode discharge through water vapor, which subsequently react with water molecules to form H_3O^+ as a reagent ion. The reaction process further continues in the source drift region, which injects the H_3O^+ cations in a purity $>99.5\%$ into the drift tube (Blake et al., 2009, IONICON, 2019).

Although ionization with H_3O^+ is an excellent technique in PTR-MS, there is one obvious limitation named proton affinity of a measured compound. On the one hand, it is desirable for the measurement of trace compounds that the main compounds of a complex gaseous sample, like CO_2 , N_2 , and O_2 , cannot be ionized due to their lower proton affinity compared to H_2O (691 kJ mol^{-1}) (Hunter & Lias, 1998). On the other, there are indeed several VOCs, where a measurement is not possible at all, due to their poor proton affinity, like small alkanes (C_1 – C_4), ethene and ethyne (Arnold et al., 1998,

IONICON, 2019). Furthermore, in cases of molecules with a slightly higher proton affinity than H_2O , like hydrogen sulfide (H_2S), hydrogen cyanide (HCN), isocyanic acid (HCNO) and formaldehyde, an equilibrium of the forward and the back-reaction is observed, which strongly depends on the humidity of the measured sample (Li et al., 2014; Moussa et al., 2016; Warneke et al., 2011; Yuan et al., 2016). In addition, there is no possibility to differentiate between carbonyl isomers, for example, aldehydes and ketones (IONICON, 2019; Jordan, Haidacher, Hanel, Hartungen, Herbig, et al., 2009). Furthermore, for alcohols and aldehydes, a loss of H_2O after the protonation (and other fragmentation processes) can be observed, which is crucial for further quantification, and lowers the overall signal for $[\text{MH}^+]$ (Buhr et al., 2002). Last but not least, based on experiences in SIFT-MS, higher alkanes ($>\text{C}_7$) are prone to fragmentation or building water-clusters (Erickson et al., 2014; Jobson et al., 2005; Španěl & Smith, 1998a, 1998b, 1998c, 1998d, 1998e). For those reasons, a PTR-MS (and SIFT-MS) analysis of a complex sample based on only the reaction with H_3O^+ as reagent ion is insufficient.

2 | NO^+ AND O_2^{+*} AS REAGENT IONS IN SIFT-MS AND PTR+SRI-MS

2.1 | General

Besides H_3O^+ , several investigations were made choosing NH_4^+ as proton donor reagent (Ellis & Mayhew, 2014), showing more association products due to three-body ion–molecule associations or ligand switching processes. Furthermore, the proton affinity of NH_3 (854 kJ mol^{-1}) is higher compared to water, resulting in lower reactivity with VOCs through proton transfer. However, a chemical ionization is not only limited to proton transfer or

association but can also occur by means of charge transfer reactions or hydride abstraction, for example with NO^+ and O_2^{+*} as reagent ions.

Both ions were already well established in SIFT-MS. The development of the proton transfer mass spectrometry, combined with switchable reagent ion capability (PTR+SRI-MS) was a major improvement for PTR-MS. Instead of using water vapor for the generation of H_3O^+ , synthetic air (N_2/O_2), O_2 or Kr is injected into the ion source (Figure 2) leading to the generation of NO^+ , O_2^{+*} , and Kr^+ , respectively (Jordan, Haidacher, Hanel, Hartungen, Herbig, et al., 2009; Sulzer et al., 2012; Wedlan & Atkinson, 2003). However, compared to SIFT-MS, switching between the different reagent ions in PTR+SRI-MS is slower and takes several seconds (Jordan, Haidacher, Hanel, Hartungen, Herbig, et al., 2009).

Whereas a reaction with Kr^+ (IE 14.00 eV) occurs with nearly every reactant leading to fragmentation due to the harsh ionization, reactions with O_2^{+*} (IE 12.07 eV) and NO^+ (IE 9.26 eV) are smoother leading to less fragmentation, and are therefore more selective (Edtbauer et al., 2014). Additionally, some research was made with CF_3^+ as a reagent (Blake et al., 2017). In the field of negative-ion PTR-MS (Veres et al., 2008), even acetate ions ($\text{CH}_3\text{C}(\text{O})\text{O}^-$) were used for the detection of mainly acids. For convenience of presentation, all ionization techniques deriving from PTR-MS, using O_2^{+*} or NO^+ as reagent ions, will be named PTR+SRI-MS, even if it is not 100% correct.

This review focusses on the chemical ionization through reactions with NO^+ and O_2^{+*} , pointing out major differences between each other in detail, and giving an overview of detected species in comparison with results from the most common reagent ion H_3O^+ . Thereby, we primarily discuss the various classes of VOCs and their behavior towards NO^+ and O_2^{+*} . Unfortunately, there is a lack of knowledge concerning NO^+ and O_2^{+*} ionization in PTR+SRI-MS in the literature. The SRI-feature is state-

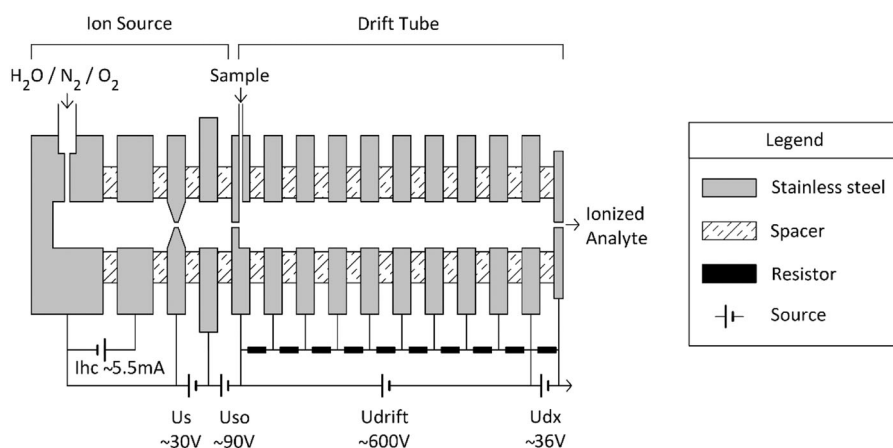
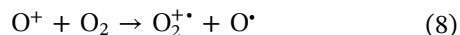
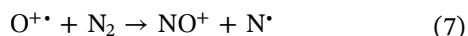
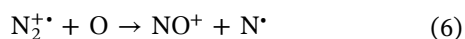
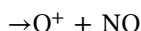
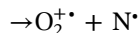
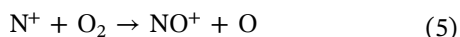
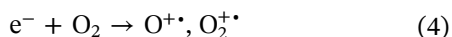
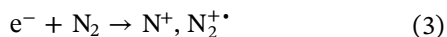


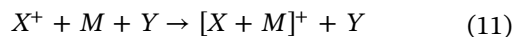
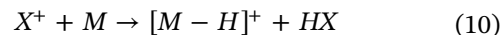
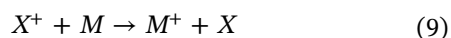
FIGURE 2 Scheme of the ion source and the drift tube in a PTR+SRI-MS according to (Blake et al., 2009; IONICON, 2019)

of-the-art, offering the possibility to measure with H_3O^+ , NO^+ , O_2^+ and even Kr^+ as reagent ions (IONICON, 2019). Therefore, most of the reported results are derived from studies using SIFT-MS as the analytical method. However, as the reaction process is similar, these studies can also contain relevant information for PTR+SRI-MS.

NO^+ ions are created by a discharge of the hollow cathode with synthetic air (N_2/O_2) or with charcoal-filtered air. As a first step, the pre-reagent ions N^+ , N_2^+ , O^+ and O_2^+ are generated, which further react in the source drift region to NO^+ (Equations 3–7) (IONICON, 2019). Unfortunately, contamination of the injected NO^+ swarm with O_2^+ is unavoidable in PTR+SRI-MS but can be minimized to be less than 2%. The formed nitrosonium ion NO^+ , a closed shell ion with an even number of electrons, is isoelectronic to CO and N_2 and exhibits a triple bond (calc. bond length $r_{\text{NO}} = 1.06 \text{ \AA}$) between nitrogen and oxygen (Holleman et al., 2007).



The dioxygenyl radical cation O_2^+ is formed in an analogous way by discharge in oxygen and further reactions in the source drift region (Equations 4 and 8). O_2^+ is a radical cation with a bond order of 2.5 ($r_{\text{OO}} = 1.12 \text{ \AA}$) (Holleman et al., 2007). Due to the configuration of the ion source, a small backflow of N_2 is unavoidable, resulting in contamination and the production of NO^+ . This amount is negligible in most of the cases, except for the usage of N_2 as a carrier gas, as NO^+ is then produced in the lower percentage range (Jordan, Haidacher, Hanel, Hartungen, Herbig, et al., 2009). Depending on the humidity of the applied gases, H_3O^+ can also appear as an impurity. Therefore, the overall purity of the O_2^+ injection is about 90%–95% (IONICON, 2019).



Considering the process in more detail, there are three possibilities for the chemical ionization via X^+ (Equation 9–11). First, a charge transfer (Equation 9), which can take place if the recombination energy of the reagent ion (NO^+ 9.26 eV; O_2^+ 12.07 eV) is higher than that of the VOC M. In the case of NO^+ , the stable radical nitrogen monoxide NO^* arises by electron abstraction, whereas dioxygen O_2 results for O_2^+ . Furthermore, the reaction enthalpy should be low enough to avoid breaking bonds within the M molecules. To avoid misunderstandings, we will name this reaction pathway charge transfer, even it is an electron abstraction/transfer, as it is the most common wording used in the literature of SIFT-MS and PTR+SRI-MS. As second pathway (Equation 10) hydride abstraction can take place if the hydride affinity of the reagent ion (NO^+ 246 kcal mol^{−1}) is larger than the hydride affinity of $[\text{M} - \text{H}]^+$. Lastly, similar to H_3O^+ , an association process is also possible (Equation 11) but is only favorable if binary reaction processes are endothermic. In SIFT-MS, this reaction pathway is both pressure and temperature dependent (Smith et al., 2001). Therefore, it is absolutely necessary to control both the temperature and the pressure of the inert carrier gas (usually He). However, in PTR+SRI-MS, this can only occur if the temperature/collision energy is low enough to avoid breaking the $[\text{X} + \text{M}]^+$ bond (IONICON, 2019). One should keep in mind, that by increasing the reduced electric field strength E/N , the development of such association products can hardly be suppressed as a consequence of the high collision energy (Edtbauer et al., 2014).

In the following section, we discuss the different compound classes, giving a table as an overview of the discussed compounds within the sections, including references to relevant literature, as well as the used method and the reagent ion (Table 1).

2.2 | Reactions with hydrocarbons

Most of the chemical ionization processes of alkanes $\text{C}_n\text{H}_{2n+2}$ with NO^+ occur via hydride abstraction, which due to the high ionization energy of alkanes, is an exothermic process compared to the endothermic charge transfer (Wedlan & Atkinson, 2003). As a result, $[\text{M} - \text{H}]^+$ and HNO are detected for most cyclic and longer chained alkanes ($m > 6$). Although a detection of propane, *n*-butane and *n*-pentane is possible, the reaction rate constants are very low, resulting in slow reactions, and

TABLE 1 Alkanes discussed in this review

Name/molecular formula	Method	Reagent ion	Literature
CH ₄ methane	SIFT-MS	O ₂ ⁺	Wilson et al. (2003)
C ₂ H ₆ ethane	SIFT-MS	O ₂ ⁺	Wilson et al. (2003)
C ₃ H ₆ cyclopropane	SIFT-MS	NO ⁺ O ₂ ⁺	Španěl and Smith (1996a)
C ₃ H ₈ propane	SIFT-MS	NO ⁺ O ₂ ⁺	Wilson et al. (2003)
C ₄ H ₁₀ <i>n</i> -butane	SIFT-MS	O ₂ ⁺	Arnold et al. (1998); Španěl and Smith (1998b); Wilson et al. (2003)
C ₄ H ₁₀ methyl propane	SIFT-MS	NO ⁺ O ₂ ⁺	Arnold et al. (1998); Španěl and Smith (1998b); Wilson et al. (2003)
C ₅ H ₁₂ <i>n</i> -pentane	SIFT-MS	NO ⁺ O ₂ ⁺	Arnold et al. (1998); Španěl and Smith (1996, 1998b)
C ₅ H ₁₂ 2-methyl butane	SIFT-MS PTR+SRI-MS	NO ⁺ O ₂ ⁺	Španěl and Smith (1998b); Koss et al. (2016)
C ₆ H ₁₂ methylcyclopentane	PTR+SRI-MS	NO ⁺	Koss et al. (2016)
C ₆ H ₁₄ <i>n</i> -hexane	SIFT-MS	NO ⁺ O ₂ ⁺	Španěl and Smith (1998b); Arnold et al. (1998)
C ₆ H ₁₄ 2-methylpentane	PTR+SRI-MS	NO ⁺	Koss et al. (2016)
C ₆ H ₁₄ 3-methylpentane	PTR+SRI-MS	NO ⁺	Koss et al. (2016)
C ₇ H ₁₆ <i>n</i> -heptane	SIFT-MS	NO ⁺	Arnold et al. (1998)
C ₇ H ₁₄ methylcyclohexane	PTR+SRI-MS	NO ⁺	Koss et al. (2016)
C ₈ H ₁₈ <i>n</i> -octane	SIFT-MS	NO ⁺ O ₂ ⁺	Španěl and Smith (1998b); Arnold et al. (1998)
C ₈ H ₁₈ <i>iso</i> -octane	SIFT-MS	NO ⁺	Arnold et al. (1998)
C ₁₀ H ₂₂ <i>n</i> -decane	SIFT-MS	NO ⁺ O ₂ ⁺	Arnold et al. (1998); Španěl and Smith (1998b)
C ₁₂ H ₂₆ <i>n</i> -dodecane	SIFT-MS	NO ⁺ O ₂ ⁺	Španěl and Smith (1998b)
C ₁₅ H ₃₂ <i>n</i> -pentadecane	PTR+SRI-MS	NO ⁺	Koss et al. (2016)
C ₁₆ H ₃₄ hexadecane	CI-MS*	NO ⁺	Hearn and Smith (2004)*

Note: Alkanes discussed in this review. If for a certain compound literature concerning both SIFT-MS and PTR+SRI-MS are given, references arising from PTR+SRI-MS are highlighted bold. In case there is no literature given regarding SIFT-MS or PTR+SRI-MS, reactions in Chemical Ionization Mass Spectrometry (CI-MS) are also mentioned here and marked with *.

impede a clear identification in a complex sample (Španěl & Smith, 1998b; Wilson et al., 2003). In contrast, the structural isomers *iso*-butane and *iso*-pentane offer high reactivity towards NO^+ . This observation is in accordance with previous results in CI-MS, as the energy barrier for hydrogen elimination on a primary carbon in saturated hydrocarbons is quite high ($\Delta H = 83.7 \text{ kJ mol}^{-1}$) (Hunt & Harvey, 1975). In addition, Arnold et al. (1998) found reasonable hints for protonated nitrosoalkanes $\text{C}_n\text{H}_{2n+1}\text{HNO}^+$ ($m = 3-5$) by the usage of N^{18}O^+ as the reagent ion (Table 2). This kind of association product is observed for longer *n*-alkanes as fragments (Španěl & Smith, 1998b), whereas the degree of fragmentation decreases with increasing chain length (Koss et al., 2016). In contrast, only little fragmentation after hydride abstraction is observed for cyclic alkanes

with NO^+ . There is indeed one exception, as *cyclo*-propane reacts by charge transfer, assumed to occur via ring opening, resulting in a propene-like C_3H_6^+ (Hunt & Harvey, 1975).

Nearly all ionization reactions involving alkanes with O_2^{+*} occur via charge transfer, usually followed by multiple fragmentation reactions, resulting in fragments like C_2H_4^+ , C_3H_7^+ , C_4H_8^+ , and so on (Table 2) (Španěl & Smith, 1998b). In many cases, the parent ion is detectable, but the signal intensity is often weaker than those of the corresponding fragments. Furthermore, the number of fragments rise with increasing number of atoms inside the molecule, resulting in complex fragmentation patterns. In contrast to NO^+ , reactions of O_2^{+*} with small hydrocarbons, $\text{C}_n\text{H}_{2n+2}$ ($m = 1-2$) take place in SIFT-MS (Wilson et al., 2003). The reaction of methane with O_2^{+*} ,

TABLE 2 Products of the reactions of NO^+ and O_2^{+*} with several aliphatic hydrocarbons in SIFT-MS

Compound	Structure	NO^+	O_2^{+*}
Methane (Hunt & Harvey, 1975, Wilson et al., 2003)		No reaction	CH_3O_2^+
Ethane (Hunt & Harvey, 1975, Wilson et al., 2003)		No reaction	C_2H_6^+ C_2H_5^+ C_2H_4^+
<i>n</i> -propane (Hunt & Harvey, 1975, Wilson et al., 2003)		C_3H_7^+	C_3H_8^+ C_3H_7^+ C_2H_5^+ C_2H_4^+
<i>n</i> -butane (Španěl & Smith, 1998b)		C_4H_9^+ (Arnold et al., 1998)	$\text{C}_4\text{H}_{10}^+$ (20) C_3H_7^+ (65) C_3H_6^+ (10) C_2H_4^+ (5)
2-methyl propane (Španěl & Smith, 1998b)		C_4H_9^+ (100)	C_4H_9^+ (25) C_4H_8^+ (10) C_3H_7^+ (40) C_3H_6^+ (25)
<i>n</i> -pentane (Španěl & Smith, 1998b)		$\text{C}_5\text{H}_{11}^+$ (>90) (Arnold et al., 1998) $\text{C}_3\text{H}_7\text{NOH}^+$ C_4H_9^+ $\text{C}_2\text{H}_5\text{NOH}^+$	$\text{C}_5\text{H}_{12}^+$ (10) C_4H_9^+ (5) C_3H_7^+ (45) C_3H_6^+ (40)
2-methyl butane (Španěl & Smith, 1998b)		$\text{C}_5\text{H}_{11}^+$ (100)	$\text{C}_5\text{H}_{12}^+$ (10) C_4H_9^+ (15) C_4H_8^+ (10) C_3H_7^+ (20) C_3H_6^+ (45)
<i>n</i> -hexane (Španěl & Smith, 1998b)		$\text{C}_6\text{H}_{13}^+$ (100)	$\text{C}_6\text{H}_{14}^+$ (20) $\sum \text{R}^+$ (45) $\sum (\text{R-H})^+$ (45)
<i>n</i> -octane (Španěl & Smith, 1998b)		$\text{C}_8\text{H}_{17}^+$ (>80) $\sum \text{RHNO}^+$ (<20)	$\text{C}_8\text{H}_{18}^+$ (30) $\sum \text{R}^+$ (40) $\sum (\text{R-H})^+$ (30)
<i>n</i> -decane (Španěl & Smith, 1998b)		$\text{C}_{10}\text{H}_{21}^+$ (>90) $\sum \text{RHNO}^+$ (<10)	$\text{C}_{10}\text{H}_{22}^+$ (35) $\sum \text{R}^+$ (45) $\sum (\text{R-H})^+$ (20)

Note: The percentage of each ion is given in brackets if known (Arnold et al., 1998; Hunt & Harvey, 1975; Španěl & Smith, 1998b; Wilson et al., 2003).

TABLE 3 Alkenes and alkynes discussed in this review

Name/molecular formula	Method	reagent ion	Literature
C ₂ H ₄ ethene	SIFT-MS PTR+SRI-MS	O ₂ ⁺ NO ⁺	Wilson et al. (2003); Cappellin et al. (2014)
C ₃ H ₆ propene	SIFT-MS	NO ⁺ O ₂ ⁺	Wilson et al. (2003)
C ₃ H ₄ propadiene	SIFT-MS	NO ⁺ O ₂ ⁺	Wilson et al. (2003)
C ₄ H ₈ 2-butene	SIFT-MS	NO ⁺ O ₂ ⁺	Wilson et al. (2003)
C ₅ H ₁₀ 1-pentene	SIFT-MS	NO ⁺ O ₂ ⁺	Španěl and Smith (1998b); Diskin et al. (2002)
C ₅ H ₁₀ trans-2-pentene	SIFT-MS	NO ⁺ O ₂ ⁺	Diskin et al. (2002)
C ₅ H ₁₀ 2-methyl 2-butene	SIFT-MS	NO ⁺ O ₂ ⁺	Španěl and Smith (1998b)
C ₅ H ₈ 2-methyl-1,3-butadiene	SIFT-MS PTR+SRI-MS	NO ⁺ O ₂ ⁺	Diskin et al. (2002); Španěl and Smith (1996a, 1998b); Koss et al. (2016); Smith et al. (2001)
C ₆ H ₁₂ 1-hexene	SIFT-MS	NO ⁺ O ₂ ⁺	Diskin et al. (2002)
C ₆ H ₁₂ trans-2-hexene	SIFT-MS	NO ⁺ O ₂ ⁺	Diskin et al. (2002)
C ₇ H ₁₄ 1-heptene	SIFT-MS	NO ⁺ O ₂ ⁺	Diskin et al. (2002)
C ₇ H ₁₄ trans-2-heptene	SIFT-MS	NO ⁺ O ₂ ⁺	Diskin et al. (2002)
C ₈ H ₁₆ 1-octene	SIFT-MS	NO ⁺ O ₂ ⁺	Diskin et al. (2002)
C ₈ H ₁₆ trans-2-octene	SIFT-MS	NO ⁺ O ₂ ⁺	Diskin et al. (2002)
C ₉ H ₁₈ 1-nonene	SIFT-MS	NO ⁺ O ₂ ⁺	Diskin et al. (2002)
C ₉ H ₁₈ trans-2-nonene	SIFT-MS	NO ⁺ O ₂ ⁺	Diskin et al. (2002)
C ₁₀ H ₂₀ 1-decene	SIFT-MS	NO ⁺ O ₂ ⁺	Diskin et al. (2002)
C ₁₀ H ₁₆ α-pinene	PTR+SRI-MS	NO ⁺	Koss et al. (2016)
C ₁₀ H ₁₆ β-pinene	SIFT-MS	NO ⁺	Spesyvyi et al. (2016)
C ₁₀ H ₁₆ 3-carene	SIFT-MS	NO ⁺	Spesyvyi et al. (2016)
C ₁₀ H ₁₆ (R)-limonene	SIFT-MS	NO ⁺	Spesyvyi et al. (2016)

(Continues)

TABLE 3 (Continued)

Name/molecular formula	Method	reagent ion	Literature
C ₁₈ H ₃₆ 1-octadecene	CI-MS*	NO ⁺	Hearn & Smith (2004)*
C ₂ H ₂ ethine	SIFT-MS	NO ⁺ O ₂ ⁺	Wilson et al. (2003)
C ₃ H ₄ propyne	SIFT-MS	NO ⁺ O ₂ ⁺	Wilson et al. (2003)
C ₄ H ₂ diacetylene	SIFT-MS	NO ⁺ O ₂ ⁺	Wilson et al. (2003)

Note: If for a certain compound literature concerning both SIFT-MS and PTR+SRI-MS are given, references arising from PTR+SRI-MS are highlighted in bold. In case there is no literature given regarding SIFT-MS or PTR+SRI-MS, reactions in Chemical Ionization Mass Spectrometry (CI-MS) are also mentioned here and marked with *.

which occurs very slowly, leads to the closed shell product ion, CH₃O₂⁺. This product, which has the same molecular structure as a hydroperoxy radical, is proposed to be generated via O₂⁺ association, further rearrangement to [CH₃O₂H]⁺ and followed by the loss of a hydrogen atom (Barlow et al., 1986; Durup-Ferguson et al., 1984; Van Doren et al., 1986). As all other reactions with small hydrocarbons proceed rapidly, but not without fragmentation, the reagent ion O₂⁺ is an essential addition for the measurement of alkanes (Table 3).

The first insights into the reaction mechanism of NO⁺ with different alkenes by chemical ionization in the gas phase were given by Hunt and Harvey (1975) demonstrating that the position of the double bond makes a significant difference on the outcome of the reaction. Based on their observations, the major product for 1-alkenes results from the electrophilic addition of NO⁺ towards the allyl group, as the latter molecule shows no reactivity in the gas phase. A Markownikoff pathway can be suggested based on calculated enthalpy changes for 1-alkenes, for example, C₈H₁₆ (Figure 3, Equations 12, 13, and 14) and the fact, that no reaction of NO⁺ is observed with ethene, leading to (C_mH_{2m-1}HNO)⁺. Besides the addition products of the full molecule (C_mH_{2m-1}HNO)⁺, several other protonated nitrosoalkenes (C_nH_{2n-1}HNO)⁺ with $n < m$ were detected for higher alkenes ($m \geq 5$). One possible explanation for their formation is a reaction mechanism including the formation of a NO-containing heterocycle, which by fragmentation leads to the development of the detected cations (Figure 3, Equation 15) (Diskin et al., 2002; Hunt & Harvey, 1975).

The association cations of the formula (C_nH_{2n-1}HNO)⁺ were also observed during SIFT-investigations of Diskin et al. (2002). However, as there is no thermochemical data available so far, these so-called insertion reactions were not further investigated. As expected,

increasing the number of atoms of 1-alkenes leads to an increasing number of protonated nitrosoalkene fragments. Interestingly, the amount of the addition product (C_mH_{2m-1}HNO)⁺ increases also by increasing the amount of atoms (Diskin et al., 2002; Liu et al., 2013). Whereas about 25% of (C₆H₁₁HNO)⁺ were detected for the reaction with 1-hexene, it is about 45% (C₁₀H₁₉HNO)⁺ for the reaction with 1-decene. This might be due to the increasing number of vibrational degrees of freedom in the excited NO-adducts, which protects the molecule against unimolecular decomposition by storing the excess of energy. For trans-2-alkenes, parallel charge transfer and hydride ion transfer are the most common reactions, whereas association processes are almost absent (Diskin et al., 2002). The charge transfer reaction is only slightly favored compared to the hydride transfer reaction, which leads to a nearly equal ratio of (C_nH_{2n})⁺ and (C_nH_{2n-1})⁺, and further opens the opportunity to distinguish between 1-alkenes and trans-2-alkenes. However, association products, as shown above for 1-alkenes and trans-2-alkenes, can be nearly excluded for PTR+SRI-MS by increasing E/N, making it more selective (Edtbauer et al., 2014). One of the most prominent VOCs, which is also a main trace component in air, is the diene isoprene C₅H₈ (Diskin et al., 2002). All three ionization pathways, charge transfer, hydride transfer and association, were observed in PTR+SRI-MS, whereas charge transfer leading to (C₅H₈)⁺ is the main pathway (Koss et al., 2016). Basically deriving from isoprene, the isomeric monoterpenes C₁₀H₁₆ β-Pinene, (S)-Limonene and 3-Carene were investigated in detail by Spesyvyi et al. (2016) with a modified SIFT-MS. Although reacting by charge transfer with NO⁺ leading to (C₁₀H₁₆)⁺ for all three isomers, they show a different fragmentation pattern by applying an additional potential with a drift tube. In total, and contrary to alkanes, the

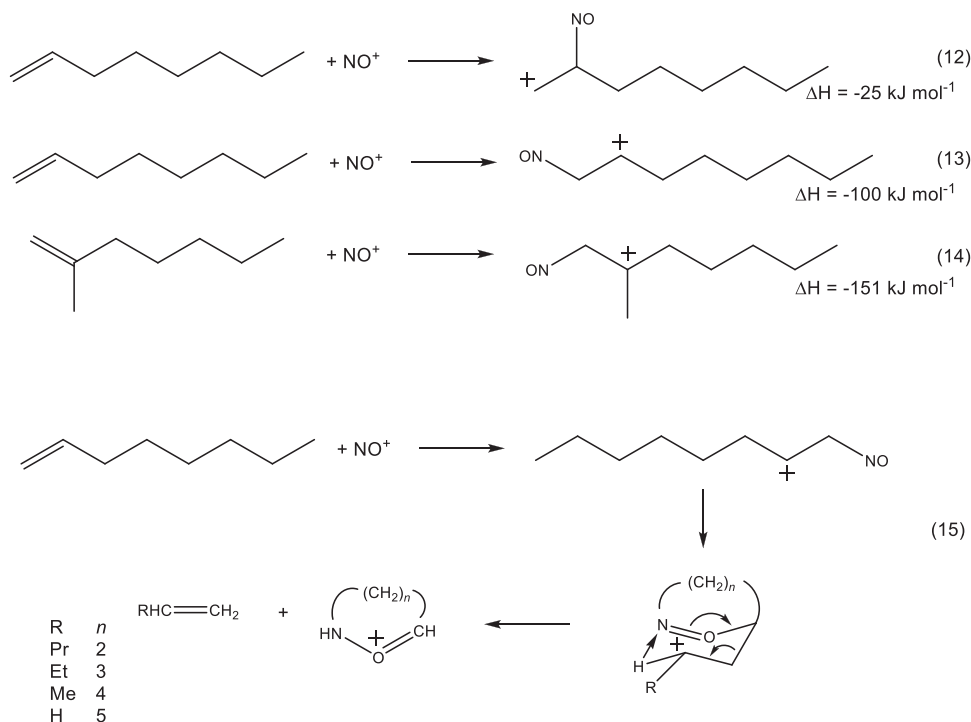


FIGURE 3 Reactions of different 1-alkenes with NO⁺ according to Diskin et al. (2002) and Hunt and Harvey (1975)

charge transfer product is the main product in most of the cases for dienes (Karl et al., 2012).

As expected, the ionization of alkenes with O₂⁺ results often in a variety of fragmentation products. However, the signal for the parent ion (C_nH_{2n})⁺ can always be detected. In contrast to NO⁺ ionization, no dependency of the mass spectra on the position of the double bond was observed. Therefore, the reactions with isomeric 1-alkenes and trans-2-alkenes yield similar product spectra (Diskin et al., 2002). All reactions proceed via charge transfer. In both, SIFT-MS and PTR+SRI-MS, only small traces of the association product of ethene (C₂H₄NO)⁺ were observed for the reaction with NO⁺ (Cappellin et al., 2014; Williams & Cool, 1991). In contrast, (C₂H₄)⁺ for SIFT-MS, and in addition (C₂H₂)⁺ for PTR+SRI-MS, were detected for O₂⁺ (Cappellin et al., 2014; Wilson et al., 2003), due to its higher ionization energy. Interestingly, (C₂H₂)⁺ becomes the dominant species at high E/N (155 Td) in PTR+SRI-MS, whereas (C₂H₄)⁺ is dominant at low E/N (94 Td). As the ionization energy of ethene is 10.51 eV (Ohno et al., 1995), a successful charge transfer reaction can only take place using O₂⁺ as a reagent ion.

Aromatic substances (Table 4), especially organic benzene derivatives, react via nondissociative charge transfer with NO⁺ as the main reaction channel in SIFT-MS (Smith et al., 2001; Španěl & Smith, 1998b). Additionally, a three-body association channel leading to (MNO)⁺ is also observed. In SIFT-MS this channel plays

a minor role for aromatic substances (<2%) other than benzene (15%) and in PTR+SRI-MS (Blake et al., 2006) it plays no role. Explanations for the special behavior of benzene are either the similar ionization energy (9.24 eV) (Nemeth et al., 1993) or a phenomenon called “charge transfer complexing,” which was also observed for some ketones. Thereby, the positive charge is delocalized around the whole molecule (C₆H₆NO)⁺ resulting in a prolonged lifetime. A charge transfer reaction is also observed for aromatics with O₂⁺. In contrast to toluene and benzene, where this reaction is solely non-dissociative in both SIFT-MS and PTR+SRI-MS, fragment cations were observed for other organic benzene derivatives (Španěl & Smith, 1998b). The main product ion for ethylbenzene, as well as for propylbenzene, is C₇H₇⁺, whereas methyl substituted derivatives show the parent ion as the main product, underlining the enhanced stability of aromatic rings compared to aliphatic hydrocarbons against fragmentation. Taking advantage of this observation, it is possible to use O₂⁺ ionization to distinguish between the two isobars xylene and ethylbenzene. Whereas xylene shows the parent ion M⁺ with about 80% and the dissociative charge transfer product (C₇H₇)⁺ with about 20%, nearly the reverse is observed for ethylbenzene (Jordan, Haidacher, Hanel, Hartungen, Herbig, et al., 2009).

Related to the complementary pathways for ionization, using NO⁺ and O₂⁺ as reagent ions, in addition to H₃O⁺, provides a great benefit in PTR+SRI-MS. Not only

TABLE 4 Aromatics discussed in this review

Name/molecular formula	Method	reagent ion	Literature
C ₆ H ₆ benzene	SIFT-MS PTR+SRI-MS	NO ⁺ O ₂ ⁺	Španěl and Smith (1996a, 1998b); Jordan, Haidacher, Hanel, Hartungen, Herbig, et al. (2009); Koss et al. (2016)
C ₇ H ₈ toluene	SIFT-MS PTR+SRI-MS	NO ⁺ O ₂ ⁺	Španěl and Smith (1996a, 1998b); Jordan, Haidacher, Hanel, Hartungen, Herbig, et al. (2009); Koss et al. (2016)
C ₈ H ₈ styrene	PTR+SRI-MS	NO ⁺	Jordan, Haidacher, Hanel, Hartungen, Herbig, et al. (2009); Koss et al. (2016)
C ₈ H ₁₀ <i>o</i> -xylene	SIFT-MS PTR+SRI-MS	NO ⁺ O ₂ ⁺	Koss et al. (2016); Španěl and Smith (1998b); Jordan, Haidacher, Hanel, Hartungen, Herbig, et al. (2009)
C ₈ H ₁₀ <i>m</i> -xylene	SIFT-MS PTR+SRI-MS	NO ⁺ O ₂ ⁺	Španěl and Smith (1998b); Jordan, Haidacher, Hanel, Hartungen, Herbig, et al. (2009)
C ₈ H ₁₀ <i>p</i> -xylene	SIFT-MS PTR+SRI-MS	NO ⁺ O ₂ ⁺	Španěl and Smith (1998b); Jordan, Haidacher, Hanel, Hartungen, Herbig, et al. (2009)
C ₈ H ₁₀ ethylbenzene	SIFT-MS PTR+SRI-MS	NO ⁺ O ₂ ⁺	Španěl and Smith (1998b); Jordan, Haidacher, Hanel, Hartungen, Herbig, et al. (2009)
C ₉ H ₁₂ propylbenzene	SIFT-MS	NO ⁺ O ₂ ⁺	Španěl and Smith (1998b)
C ₉ H ₁₂ 1,2,4-trimethylbenzene	SIFT-MS PTR+SRI-MS	NO ⁺	Koss et al. (2016); Španěl and Smith (1998b); Jordan, Haidacher, Hanel, Hartungen, Herbig, et al., (2009)
C ₉ H ₁₂ 1,2,3-trimethylbenzene	SIFT-MS PTR+SRI-MS	NO ⁺ O ₂ ⁺	Španěl and Smith (1998b); Jordan, Haidacher, Hanel, Hartungen, Herbig, et al., (2009)
C ₉ H ₁₂ 1,3,5-trimethylbenzene	SIFT-MS PTR+SRI-MS	NO ⁺ O ₂ ⁺	Španěl and Smith (1998b); Jordan, Haidacher, Hanel, Hartungen, Herbig, et al. (2009)

Note: If for a certain compound literature concerning both SIFT-MS and PTR+SRI-MS are given, references arising from PTR+SRI-MS are highlighted in bold. In case there is no literature given regarding SIFT-MS or PTR+SRI-MS, reactions in Chemical Ionization Mass Spectrometry (CI-MS) are also mentioned here and marked with *.

the range of detectable alkanes is expanded towards smaller ones, for example, C₅ and C₄- alkanes in SIFT-MS (Španěl & Smith, 1998b), but also NO⁺ offers the possibility to detect larger *n*-alkanes (≥C₁₂) with far less fragmentation compared to H₃O⁺ (Erickson et al., 2014, Koss et al., 2016). Furthermore, isomeric aromatic compounds, for example, xylene and ethylbenzene, can be distinguished with O₂⁺ through their different reaction ratios in PTR+SRI-MS, whereas only the molecular ion peak is observed for both NO⁺ and H₃O⁺ (Jordan, Haidacher, Hanel, Hartungen, Herbig, et al., 2009).

2.3 | Reactions with alcohols

Besides pure hydrocarbons, oxygen containing species, especially alcohols (Table 5), are of major interest as VOCs in different fields of research (Hlastala, 1998, M. Coelho Neto et al., 2020). Depending on the position of the OH-group, primary, secondary, and tertiary alcohols exhibit a variety of reactions with NO⁺ in the gas phase (Hearn & Smith, 2004, Hunt et al., 1982, Smith, Diskin, Ji, Španěl 2001, Španěl & Smith, 1997, Španěl

et al., 2017). Early investigations in CI-MS (Hunt et al., 1982) showed the association product [MNO]⁺, the hydride abstraction products [M-H]⁺, [M-3H]⁺ and [MNO-2H]⁺, as well as the hydroxide abstraction product [M-OH]⁺. The association product [CH₄ONO]⁺ results from a three-body collision of methanol, NO⁺ and the carrier gas (He) in SIFT-MS (Table 6). However, due to the low reaction rate of about 1%, a quantification is not expedient and a qualitative verification is only barely feasible in complex gas mixtures (Španěl et al., 2017). The reactions of ethanol and the two propanol isomers occur primary via hydride abstraction on a carbon atom, which is in accordance with the given thermodynamic data (Smith, Diskin, Ji, Španěl 2001, Španěl & Smith, 1997). Additionally, for ethanol (7%) and 1-propanol (4%), the association product [MNO]⁺ is observed, too (Španěl et al., 2017). Hydroxide transfer reaction according to Equation (16) proceeds first with the tertiary alcohol 2-methyl-2-propanol, C₄H₉OH, whereas the other isomeric C₄-alcohol reacts mainly via hydride abstraction.

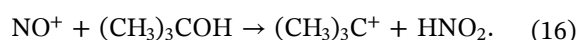


TABLE 5 Alcohols discussed in this review

Name/molecular formula	Method	reagent ion	Literature
CH ₃ OH methanol	SIFT-MS PTR+SRI-MS	NO ⁺ O ₂ ⁺	Španěl and Smith (1997); Španěl et al. (2017); Koss et al. (2016); Španěl and Smith (1996a)
C ₂ H ₅ OH ethanol	SIFT-MS PTR+SRI-MS	NO ⁺ O ₂ ⁺	Španěl and Smith (1996a); Smith et al. (2001); Španěl and Smith (1997); Španěl et al. (2017); Koss et al. (2016)
C ₃ H ₇ OH 1-propanol	SIFT-MS	NO ⁺ O ₂ ⁺	Smith et al. (2001); Španěl et al. (2017)
C ₃ H ₇ OH 2-propanol	SIFT-MS	NO ⁺ O ₂ ⁺	Španěl and Smith (1997)
C ₄ H ₉ OH 1-butanol	SIFT-MS	NO ⁺ O ₂ ⁺	Španěl and Smith (1997); Španěl et al. (2017)
C ₄ H ₉ OH 2-butanol	SIFT-MS	NO ⁺ O ₂ ⁺	Španěl and Smith (1997)
C ₄ H ₉ OH 2-methyl-1-propanol	SIFT-MS	NO ⁺ O ₂ ⁺	Španěl and Smith (1997)
C ₄ H ₉ OH 2-methyl-2-propanol	SIFT-MS	NO ⁺ O ₂ ⁺	Španěl and Smith (1997)
C ₅ H ₉ OH 1-penten-3-ol	SIFT-MS	NO ⁺ O ₂ ⁺	Schoon et al. (2007)
C ₅ H ₉ OH <i>cis</i> -2-penten-1-ol	SIFT-MS	NO ⁺ O ₂ ⁺	Schoon et al. (2007)
C ₅ H ₉ OH <i>trans</i> -2-penten-1-ol	SIFT-MS	NO ⁺ O ₂ ⁺	Schoon et al. (2007)
C ₅ H ₉ OH 2-methyl-3-buten-2-ol	SIFT-MS	NO ⁺ O ₂ ⁺	Amelynck et al. (2005)
C ₅ H ₉ OH 3-methyl-2-buten-1-ol	SIFT-MS	NO ⁺ O ₂ ⁺	Schoon et al. (2007)
C ₅ H ₉ OH 3-methyl-3-buten-1-ol	SIFT-MS	NO ⁺ O ₂ ⁺	Schoon et al. (2007)
C ₅ H ₉ OH 3-methyl-2-buten-2-ol	SIFT-MS	NO ⁺ O ₂ ⁺	Schoon et al. (2007)
C ₅ H ₁₁ OH 1-pentanol	SIFT-MS	NO ⁺ O ₂ ⁺	Španěl and Smith (1997); Španěl et al. (2017)
C ₅ H ₁₁ OH 3-pentanol	SIFT-MS	NO ⁺ O ₂ ⁺	Španěl and Smith (1997)
C ₅ H ₁₁ OH 3-methyl-1-butanol	SIFT-MS	NO ⁺ O ₂ ⁺	Španěl and Smith (1997)
C ₅ H ₁₁ OH 2-methyl-2-butanol	SIFT-MS	NO ⁺ O ₂ ⁺	Španěl and Smith (1997)
C ₆ H ₅ OH phenol	SIFT-MS PTR+SRI-MS	NO ⁺ O ₂ ⁺	Španěl and Smith (1997); Romano and Hanna (2018)
C ₆ H ₄ (OH) ₂ 2-hydroxyl phenol	SIFT-MS	NO ⁺ O ₂ ⁺	Wang et al. (2004)
C ₆ H ₁₁ OH <i>cis</i> -2-hexen-1-ol	SIFT-MS	NO ⁺ O ₂ ⁺	Schoon et al. (2007)

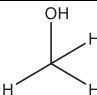
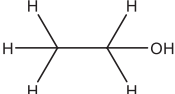
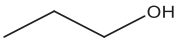
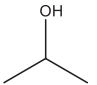
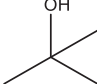
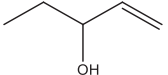
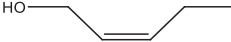
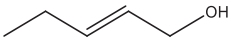
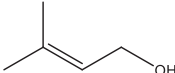
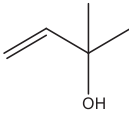
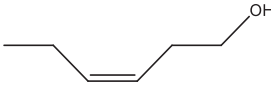
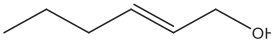
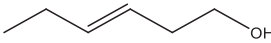
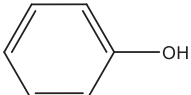
(Continues)

TABLE 5 (Continued)

Name/molecular formula	Method	reagent ion	Literature
C ₆ H ₁₁ OH <i>trans</i> -2-hexen-1-ol	SIFT-MS	NO ⁺ O ₂ ⁺	Schoon et al. (2007)
C ₆ H ₁₁ OH <i>cis</i> -3-hexen-1-ol	SIFT-MS	NO ⁺ O ₂ ⁺	Amelynck et al. (2005)
C ₆ H ₁₁ OH <i>trans</i> -3-hexen-1-ol	SIFT-MS	NO ⁺ O ₂ ⁺	Schoon et al. (2007)
C ₆ H ₁₃ OH 1-hexanol	SIFT-MS	NO ⁺ O ₂ ⁺	Španěl and Smith (1997); Španěl et al. (2017)
C ₇ H ₇ OH 2-methyl phenol	SIFT-MS	NO ⁺ O ₂ ⁺	Wang et al. (2004)
C ₇ H ₇ OH 3-methyl phenol	SIFT-MS	NO ⁺ O ₂ ⁺	Wang et al. (2004)
C ₇ H ₇ OH 4-methyl phenol	SIFT-MS PTR+SRI-MS	NO ⁺ O ₂ ⁺	Wang et al. (2004); Romano and Hanna (2018)
C ₇ H ₇ OH phenyl methanol	SIFT-MS	NO ⁺ O ₂ ⁺	Wang et al. (2004)
C ₈ H ₉ OH 4-ethyl phenol	SIFT-MS PTR+SRI-MS	NO ⁺ O ₂ ⁺	Wang et al. (2004); Romano and Hanna (2018)
C ₈ H ₉ OH 1-phenyl ethanol	SIFT-MS	NO ⁺ O ₂ ⁺	Wang et al. (2004)
C ₈ H ₉ OH 2-phenyl ethanol	SIFT-MS	NO ⁺ O ₂ ⁺	Wang et al. (2004)
C ₈ H ₁₅ OH 1-octen-3-ol	SIFT-MS	NO ⁺ O ₂ ⁺	Schoon et al. (2007)
C ₈ H ₁₅ OH DL-6-methyl-5-hepten-2-ol	SIFT-MS	NO ⁺ O ₂ ⁺	Schoon et al. (2007)
C ₈ H ₁₇ OH 1-octanol	SIFT-MS	NO ⁺ O ₂ ⁺	Španěl and Smith (1997)
C ₈ H ₁₇ OH 2-octanol	SIFT-MS	NO ⁺ O ₂ ⁺	Španěl and Smith (1997)
C ₁₀ H ₁₇ OH linalool	SIFT-MS	NO ⁺ O ₂ ⁺	Amelynck et al. (2005)
C ₁₀ H ₁₇ OH nerol	SIFT-MS	NO ⁺ O ₂ ⁺	Amelynck et al. (2005)
C ₁₀ H ₁₇ OH geraniol	SIFT-MS	NO ⁺ O ₂ ⁺	Amelynck et al. (2005)
C ₁₀ H ₁₉ OH menthol	SIFT-MS	NO ⁺ O ₂ ⁺	Španěl and Smith (1997)
C ₁₀ H ₂₁ OH decyl alcohol	CI-MS*	NO ⁺	Hearn and Smith (2004)*
C ₁₈ H ₃ OH oleyl alcohol	CI-MS*	NO ⁺	Hearn and Smith (2004)*

Note: If for a certain compound literature concerning both SIFT-MS and PTR+SRI-MS are given, references arising from PTR+SRI-MS are highlighted in bold. In case there is no literature given regarding SIFT-MS or PTR+SRI-MS, reactions in Chemical Ionization Mass Spectrometry (CI-MS) are also mentioned here and marked with *.

TABLE 6 Reactions of selected alcohols with NO⁺ and O₂⁺ in SIFT-MS

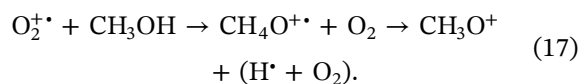
Compound	Structure	NO ⁺	O ₂ ⁺
Methanol		(CH ₄ ONO) ⁺ (100)	CH ₃ O ⁺ (50) CH ₄ O ⁺ (50)
Ethanol (Španěl & Smith, 1997; Španěl et al., 2017)		C ₂ H ₅ O ⁺ (93) (C ₂ H ₅ ONO) ⁺ (7)	C ₂ H ₅ O ⁺ (75) C ₂ H ₆ O ⁺ (25)
1-Propanol (Španěl & Smith, 1997; Španěl et al., 2017)		C ₃ H ₇ O ⁺ (96) (C ₃ H ₇ ONO) ⁺ (4)	CH ₃ O ⁺ (90) C ₃ H ₆ ⁺ (10)
2-Propanol		C ₃ H ₇ O ⁺ (100)	C ₂ H ₅ O ⁺ (100)
2-Methyl-2-propanol		C ₄ H ₉ ⁺ (100)	C ₃ H ₇ O ⁺ (100)
1-Penten-3-ol		C ₃ H ₅ O ⁺ (5) C ₅ H ₉ ⁺ (37) C ₅ H ₉ O ⁺ (56) others (2)	C ₃ H ₅ O ⁺ (75) C ₄ H ₇ O ⁺ (2) C ₅ H ₁₀ O ⁺ (13) Others (10)
cis-2-Penten-1-ol		C ₅ H ₈ ⁺ (4) C ₅ H ₉ ⁺ (24) C ₅ H ₉ O ⁺ (68) C ₅ H ₁₀ O ⁺ (4)	C ₂ H ₄ O ⁺ (7) C ₃ H ₄ O ⁺ (3) C ₃ H ₅ O ⁺ (56) C ₅ H ₈ ⁺ (15) C ₄ H ₇ O ⁺ (4) C ₅ H ₁₀ O ⁺ (9) others (6)
trans-2-Penten-1-ol		C ₅ H ₉ ⁺ (31) C ₅ H ₉ O ⁺ (58) C ₅ H ₁₀ O ⁺ (8) others (3)	C ₂ H ₄ O ⁺ (7) C ₃ H ₄ O ⁺ (5) C ₃ H ₅ O ⁺ (62) C ₅ H ₈ (5) C ₄ H ₇ O ⁺ (3) C ₅ H ₁₀ O ⁺ (13) others (5)
3-Methyl-2-buten-1-ol		C ₅ H ₉ ⁺ (40) C ₄ H ₇ O ⁺ (2) C ₅ H ₉ O ⁺ (22) C ₅ H ₁₀ O ⁺ (35) others (1)	C ₅ H ₈ ⁺ (7) C ₄ H ₇ O ⁺ (80) C ₅ H ₁₀ O ⁺ (9) others (4)
2-Methyl-3-buten-2-ol		C ₅ H ₉ ⁺ (96) others (4)	C ₃ H ₇ O ⁺ (10) C ₅ H ₉ ⁺ (2) C ₄ H ₇ O ⁺ (71) C ₅ H ₁₀ O ⁺ (8) others (9)
cis-2-Hexen-1-ol		C ₆ H ₁₀ ⁺ (7) C ₆ H ₁₁ ⁺ (23) C ₆ H ₁₁ O ⁺ (61) C ₆ H ₁₂ O ⁺ (4) others (5)	C ₂ H ₄ O ⁺ (5) C ₃ H ₄ O ⁺ (5) C ₃ H ₅ O ⁺ (36) C ₅ H ₇ ⁺ (8) C ₄ H ₇ O ⁺ (5) C ₄ H ₈ O ⁺ (3) C ₆ H ₁₀ ⁺ (23) C ₆ H ₁₂ O ⁺ (3) others (12)
trans-2-Hexen-1-ol		C ₆ H ₁₁ ⁺ (31) C ₆ H ₁₁ O ⁺ (55) C ₆ H ₁₂ O ⁺ (10) others (4)	C ₂ H ₄ O ⁺ (6) C ₃ H ₄ O ⁺ (5) C ₃ H ₅ O ⁺ (44) C ₅ H ₇ ⁺ (5) C ₄ H ₇ O ⁺ (7) C ₄ H ₈ O ⁺ (4) C ₆ H ₁₀ ⁺ (15) C ₆ H ₁₂ O ⁺ (5) others (9)
trans-3-Hexen-1-ol		C ₄ H ₈ O ⁺ (4) C ₆ H ₁₀ ⁺ (25) C ₆ H ₁₁ O ⁺ (31) C ₆ H ₁₂ O ⁺ (34) others (6)	C ₃ H ₅ O ⁺ (3) C ₅ H ₇ ⁺ (19) C ₅ H ₉ ⁺ (12) C ₅ H ₁₀ ⁺ (12) C ₆ H ₁₀ ⁺ (38) others (16)
Phenol		C ₆ H ₆ O ⁺ (100)	C ₆ H ₆ O ⁺ (100)

Note: Percentage is given in brackets (Hearn & Smith, 2004; Hunt et al., 1982; Schoon et al., 2007; Španěl & Smith, 1997; Španěl et al., 2017).

This type of reaction, which is known for several decades in nitric oxide reactions (Hunt & Ryan, 1972; Williamson & Beauchamp, 1974) is strongly favored for two reasons. First, no α -hydrogen is available for hydride abstraction, and second, the resulting tertiary carbocation $(\text{CH}_3)_3\text{C}^+$ is stabilized by the inductive effect of three methyl groups. A similar observation is made for the reactions of the isomers of $\text{C}_5\text{H}_{11}\text{OH}$ with NO^+ , in which the hydroxide transfer is the only reaction pathway for 2-methyl-2-butanol, whereas it only corresponds to a minor role in 3-methyl-1-butanol and 3-pentanol and none in 1-pentanol (Španěl & Smith, 1997). Therefore, it is easy to assume that tertiary alcohols react almost exclusively via hydroxide transfer with NO^+ . On the contrary, this reaction pathway is negligible for primary alcohols, as the dominant route is hydride transfer. In the case of secondary alcohols, a mixture of both, hydroxide transfer and hydride transfer, is observed, where the latter is the main contribution. Interestingly, in case of the monoterpene alcohol menthol $\text{C}_{10}\text{H}_{19}\text{OH}$, which is formally a secondary alcohol, the mixture is comprised of equal shares. The resulting hydride abstraction products $[\text{M}-\text{H}]^+$ have a high dependency on humidity, and are often observed for polar analytes. Španěl et al. (2017) demonstrated, by variation of the absolute humidity up to 5.5%, the formation of different water clusters $[\text{M}-\text{H}]^+(\text{H}_2\text{O})_{1/2/3}$ in SIFT-MS. The first cluster is primarily formed, while the third and the second clusters are only observed in low percentages. As shown by Schoon et al. (2007), unsaturated alcohols offer hydride transfer, hydroxide transfer, and charge transfer as reaction channels (Table 6). Hydride transfer is often the main pathway for compounds having the double bond and the OH-group in position 1 and 2, respectively, like *cis*-2-penten-1-ol and *trans*-2-hexen-1-ol. With increasing distance between the functional groups, charge transfer reactions gain more importance. For example, in the case of *trans*-2-hexen-1-ol, about 10% of the ionizations proceed via charge transfer, whereas *trans*-3-hexen-1-ol takes this route about 34% of the time. Furthermore, the level of chain branching plays an important role. For instance, 2-methyl-3-buten-2-ol reacts nearly exclusively via hydroxide abstraction. However, it is not possible to frame an obvious general trend for the reaction of unsaturated alcohols with NO^+ .

In analogy to aromatic compounds, phenol and its derivatives react via nondissociative charge transfer with NO^+ leading to M^+ , including a lower ionization energy of these compounds than 9.26 eV (Španěl & Smith, 1997; Wang et al., 2004). Charge transfer is also the major process when the OH-substituent is next to the aromatic group, for example, 1-phenylmethanol or 2-phenylethanol. However, hydride and hydroxide transfer are also observed

as reaction pathways in SIFT-MS (Wang et al., 2004). In comparison, the reactions with O_2^+ result mainly in the charge transfer product. Interestingly, for methanol both, CH_4O^+ and CH_3O^+ , are observed in a nearly equal ratio in SIFT-MS (Španěl & Smith, 1997). Whereas the CH_4O^+ is generated by charge transfer, one might assume that CH_3O^+ is created via hydride transfer. However, this is not the case, and can be explained by a following hydrogen transfer from the initial charge transfer product CH_4O^+ (Equation 17). This phenomenon is also observed for ethanol, leading to $\text{C}_2\text{H}_6\text{O}^+$ and $\text{C}_2\text{H}_5\text{O}^+$, with an exceeding abundance of $\text{C}_2\text{H}_5\text{O}^+$. Furthermore, CH_3O^+ is detected as fragmentation product (Smith, Diskin, Ji, Španěl 2001, Španěl & Smith, 1997).



In case of the isomeric alcohols, 1-propanol and 2-propanol, O_2^+ can be utilized to distinguish between both (Španěl & Smith, 1997). Whereas $\text{C}_2\text{H}_5\text{O}^+$ is observed exclusively for 2-propanol, only CH_3O^+ as major and C_3H_6^+ as minor fragmentation products are detected for 1-propanol. Another interesting observation was made as a result of the reaction of the tertiary alcohol $(\text{CH}_3)_3\text{COH}$ with O_2^+ leading to a single signal resulting from $\text{C}_3\text{H}_7\text{O}^+$ (Španěl & Smith, 1997). With increasing chain length, the fragmentation patterns become more complex, similar to those obtained from electron ionization. Nevertheless, O_2^+ ionization is still useful to differ between certain isomers, as the positioning of the functional OH-group leads to different fragmentation patterns.

For primary alcohols, hydrocarbon ions are observed in most of the cases, in contrast to the carboxy ions produced within the reactions of secondary and tertiary alcohols (Španěl & Smith, 1997). Carboxy ions tend to hydrate, which further facilitates fragmentation, especially in humid samples (Španěl et al., 2017). No enhanced stability is observed for nonaromatic, cyclic alcohols, for example, the reaction with menthol results multiple fragmentation through dissociative charge transfer. All reactions of O_2^+ with unsaturated alcohols proceed through exothermic charge transfer, followed by multiple fragmentations, resulting in a variety of different cations in SIFT-MS (Amelynck et al., 2005; Schoon et al., 2007). No clear tendency is observed in all reactions with NO^+ ionization. Every single compound has to be considered in detail. Aromatic alcohols exhibit high stability, whereby no fragmentation is observed for phenol and methyl-substituted phenols after charge transfer, but only the parent ion M^+ can be detected (Wang et al., 2004). However, by increasing the chain length of

TABLE 7 Aldehydes discussed in this review

Name/molecular formula	Method	reagent ion	Literature
H ₂ CO formaldehyde	SIFT-MS	NO ⁺ O ₂ ⁺	Španěl et al. (1997)
C ₂ H ₄ O acetaldehyde	SIFT-MS PTR+SRI-MS	NO ⁺ O ₂ ⁺	Španěl et al. (1997); Španěl and Smith (1996a); Smith et al. (2014); Mochalski et al. (2014a); Koss et al. (2016)
C ₃ H ₄ O acrolein	SIFT-MS PTR+SRI-MS	NO ⁺ O ₂ ⁺	Španěl et al. (1997); Jordan, Haidacher, Hanel, Hartungen, Herbig, et al. (2009); Mochalski et al. (2014a)
C ₃ H ₆ O propanal	SIFT-MS PTR+SRI-MS	NO ⁺ O ₂ ⁺	Španěl et al. (1997); Jordan, Haidacher, Hanel, Hartungen, Herbig, et al. (2009); Mochalski et al. (2014a)
C ₄ H ₆ O methacrolein	PTR+SRI-MS	NO ⁺	Koss et al. (2016)
C ₄ H ₆ O crotonaldehyde	PTR+SRI-MS	NO ⁺	Jordan, Haidacher, Hanel, Hartungen, Herbig, et al. (2009); Mochalski et al. (2014a)
C ₄ H ₈ O <i>iso</i> -butanal	PTR+SRI-MS	NO ⁺	Mochalski et al. (2014a)
C ₄ H ₈ O <i>n</i> -butanal	SIFT-MS PTR+SRI-MS	NO ⁺ O ₂ ⁺	Smith et al. (2014); Španěl et al. (1997); Wyche et al. (2005); Mochalski et al. (2014a)
C ₅ H ₄ O ₂ furfural	PTR+SRI-MS	NO ⁺	Mochalski et al. (2014a)
C ₅ H ₈ O 2-methyl-2-butanal	PTR+SRI-MS	NO ⁺	Mochalski et al. (2014a)
C ₅ H ₈ O 2-methyl-3-butanal	PTR+SRI-MS	NO ⁺	Mochalski et al. (2014a)
C ₅ H ₈ O <i>trans</i> -2-pentenal	SIFT-MS	NO ⁺ O ₂ ⁺	Smith et al. (2014)
C ₅ H ₈ O ₂ 1,5-pentanedial	SIFT-MS	NO ⁺ O ₂ ⁺	Španěl et al. (1997)
C ₅ H ₁₀ O different pentanals	SIFT-MS PTR+SRI-MS	NO ⁺ O ₂ ⁺	Smith et al. (2014); Španěl et al. (1997); Mochalski et al. (2014a)
C ₆ H ₁₀ O <i>trans</i> -2-hexenal	SIFT-MS	NO ⁺ O ₂ ⁺	Španěl et al. (1997)
C ₆ H ₁₀ O <i>cis</i> -3-hexenal	SIFT-MS	NO ⁺ O ₂ ⁺	Španěl et al. (1997)
C ₆ H ₁₂ O <i>n</i> -hexanal	CI-MS* SIFT-MS PTR+SRI-MS	NO ⁺ O ₂ ⁺	Hearn and Smith (2004)*; Smith et al. (2014); Španěl et al. (1997); Wyche et al. (2005)
C ₇ H ₁₄ O <i>n</i> -heptanal	SIFT-MS PTR+SRI-MS	NO ⁺ O ₂ ⁺	Romano and Hanna (2018); Smith et al. (2014); Mochalski et al. (2014a)
C ₇ H ₆ O benzaldehyde	SIFT-MS PTR+SRI-MS	NO ⁺ O ₂ ⁺	Smith et al. (2014); Španěl et al. (1997); Mochalski et al. (2014a)
C ₈ H ₁₄ O <i>trans</i> -2-octenal	SIFT-MS	NO ⁺ O ₂ ⁺	Smith et al. (2014)
C ₈ H ₁₆ O 2-ethyl-hexanal	PTR+SRI-MS	NO ⁺	Mochalski et al. (2014a)
C ₈ H ₁₆ O <i>n</i> -octanal	CI-MS* SIFT-MS PTR+SRI-MS	NO ⁺ O ₂ ⁺	Hearn and Smith (2004)*; Smith et al. (2014); Romano and Hanna (2018), Mochalski et al. (2014a)

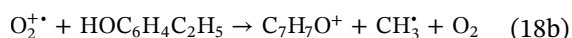
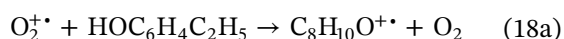
(Continues)

TABLE 7 (Continued)

Name/molecular formula	Method	reagent ion	Literature
C ₉ H ₁₈ O <i>n</i> -nonanal	SIFT-MS PTR+SRI-MS	NO ⁺ O ₂ ⁺	Smith et al. (2014); Romano and Hanna (2018); Mochalski et al. (2014a)
C ₁₀ H ₂₀ O <i>n</i> -decanal	SIFT-MS PTR+SRI-MS	NO ⁺ O ₂ ⁺	Smith et al. (2014); Romano and Hanna (2018); Mochalski et al. (2014a)
C ₁₁ H ₂₀ O 2-undecenal	PTR+SRI-MS	NO ⁺	Mochalski et al. (2014a)
C ₁₁ H ₂₂ O <i>n</i> -undecanal	SIFT-MS PTR+SRI-MS	NO ⁺ O ₂ ⁺	Smith et al. (2014); Mochalski et al. (2014a)

Note: If for a certain compound literature concerning both SIFT-MS and PTR+SRI-MS are given, references arising from PTR+SRI-MS are highlighted in bold. In case there is no literature given regarding SIFT-MS or PTR+SRI-MS, reactions in Chemical Ionization Mass Spectrometry (CI-MS) are also mentioned here and marked with *.

the aliphatic substituent, fragmentation takes place. Both, the parent ion C₈H₁₀O⁺ and the fragment ion C₇H₇O⁺ were determined for the reaction of 4-Ethylphenol, whereby the latter contributes to about 60% (Equation 18) of the products. Regarding alcohols substituted with a phenyl group, the observation switches completely, as a multitude of fragment ions are detected, for example, for phenylmethanol and phenylethanol.



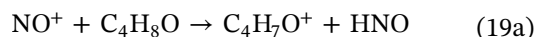
Overall, charge transfer reactions of NO⁺ or O₂⁺ with alcohols are more informative than proton transfer reactions based on H₃O⁺. First, aliphatic alcohols larger than C₃ undergo mainly H₂O elimination after protonation, resulting in (MH-H₂O)⁺ and leading to a danger of confusion with cyclic carbohydrates (Schoon et al., 2007, Španěl & Smith, 1997, Španěl et al., 2017). Second, reactions with H₃O⁺ in humid samples result a broader product ion distribution, including not only monohydrated complexes, but also a higher amount of di- and tri-hydrated association ions, depending on the degree of humidity (Španěl et al., 2017). Both can be avoided using NO⁺ or O₂⁺ as the reagent ion.

2.4 | Reactions with aldehydes and ketones

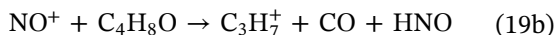
Formaldehyde, being the most simple aldehyde, shows no reaction with NO⁺ due to the high ionization energy (10.88 eV) and an endothermic hydride transfer (Haynes et al., 2016-2017). All other aldehydes (Table 7), saturated as well as unsaturated, feature hydride transfer as the dominant reaction channel in SIFT-MS (Španěl

et al., 1997). Furthermore, association products are detected as minor products (Smith et al., 2014). Similar observations are made in PTR+SRI-MS (Mochalski et al., 2014a). In addition to hydride transfer and association products, hydrocarbon ions are often observed. As mentioned earlier, association products (MNO)⁺ are produced via a three-body reaction as the excited intermediate (MNO)⁺ is stabilized by collision with a buffer gas particle (e.g., N₂, He). However, these products are only observed for unsaturated alkanals, and amount to just a few percent. For most of the alkanals, the major percentage is covered by the hydride transfer products (M-H)⁺ according to Equation (19a), which offers the possibility to differentiate them from isomeric ketones, where the association product is mainly observed (Španěl et al., 1997). Regarding *n*-alkanals, an interesting phenomenon is observed. With increasing number of atoms, the percentage of (M-H)⁺ pass through a minimum value at both dry and humid (AH 3.5%) conditions. Starting with 100% for acetaldehyde, a minimum of 13% is observed for *n*-hexanal, before the value increases again for heavier alkanals. Heavier alkanals exhibit less fragmentation, for example, *n*-undecanal, which exhibits about 85% (M-H)⁺ (Mochalski et al., 2014a). A possible explanation is the larger number of vibrational modes with increasing atomativity, which split the excess amount of energy. Additionally, there are other competing exothermic reaction channels (Equation 19a), whose share increases with less exothermicity of the hydride transfer. Furthermore, due to the detection of closed shell hydrocarbon ions (C_mH_{2m+1})⁺, a fragmentation process, including the elimination of a neutral CO molecule of the hydride abstraction product (M-H)⁺, can be assumed (Equation 19b). Mochalski et al. (2014a) have proven this assumption for C₃–C₇ alkanals. The addition of humidity to the sample increases the number of reaction channels

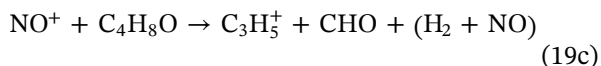
even further, leading to (M+H)⁺ (Equation 19g) and (M+H-H₂O)⁺ (Equation 19h) as detected side products.



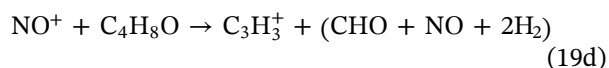
(Mochalski et al., 2014a; Wyche et al., 2005)



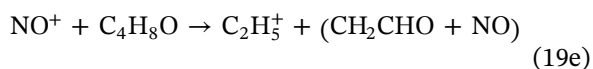
(Mochalski et al., 2014a; Wyche et al., 2005)



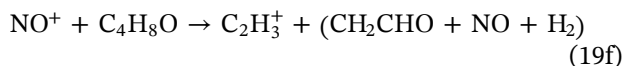
(Mochalski et al., 2014a; Wyche et al., 2005)



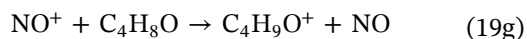
(Mochalski et al., 2014a; Wyche et al., 2005)



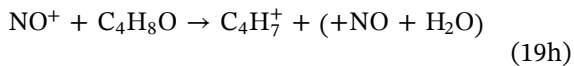
(Wyche et al., 2005)



(Wyche et al., 2005)



(Wyche et al., 2005)

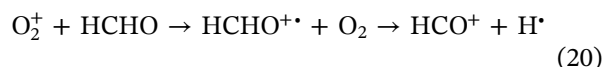


(Wyche et al., 2005)

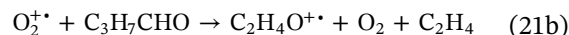
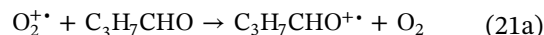
In addition to the discussed reaction channels for alkanals, charge transfer can also take place, leading to M⁺. Even if observed only in small amounts in PTR+SRI-MS, this behavior is somehow unexpected, as the ionization energies for most of the aldehydes and ketones are greater than that of NO⁺. This is especially the case for smaller molecules (Wyche et al., 2005). An explanation can be given by considering the instrument structure of a PTR+SRI-MS. The ionization energy difference can be compensated for by translational energy, which is provided to the ions by the electrical field along the drift tube. An exception is furfural (C₅H₄O₂, IE 9.22 eV) (Klapstein et al., 1990), which shows (C₅H₄O₂)⁺ as a major product due to the similar ionization energy to NO⁺ (Table 8).

Overall, a higher percentage of association complexes is found for ketones than for aldehydes in PTR+SRI-MS and SIFT-MS (Smith et al., 2019). Furthermore, and contrary to SIFT-MS, a high degree of fragmentation is observed for ketones in PTR+SRI-MS with NO⁺. Thus, the produced characteristic fragmentation patterns lay the foundation for the identification of isomeric ketones, for example, 2-hexanone and 3-hexanone. The dominant, and in many cases, only reaction product in SIFT-MS is the association product (MNO)⁺ which makes the mass spectra less complex, but hinders the possibility to differentiate between the isomers. However, there are exceptions, like 3-hexanone (C₆H₁₂O), menthone (C₁₀H₁₈O) (Španěl et al., 1997) and also diones like 2,3-pentanedione (C₅H₈O₂) (Smith et al., 2019), which (partially) react through charge transfer, resulting in the detection of M⁺.

Contrary to NO⁺, it is possible to measure formaldehyde using O₂⁺ as the reagent ion. The reaction, as all reactions with aldehydes, proceeds via charge transfer followed by fragmentation in SIFT-MS (Equation 20) (Španěl et al., 1997).



The percentage of the fragment ion(s) increases with increasing number of atoms. While the parent ion is the major product for formaldehyde (60%), it accounts for half of the fragmentation (30%) for 1-propanal (C₂H₅CHO), and is not observed anymore for 1-pentanal (C₄H₉CHO). A loss of a hydrogen atom is observed leading to (M-H)⁺ as fragment ions, as in formaldehyde, acetaldehyde and 1-propanal. The reaction channel switches for 1-butanal resulting in (C₂H₄O)⁺ as the major product, and the only observed fragment besides M⁺ (Equation 21).



Another reaction channel is the loss of “HCO,” which was observed for the alkenals 2-hexenal and 3-hexenal (Španěl et al., 1997). Again, aromatic compounds show enhanced stability against extensive fragmentation. The reaction of benzaldehyde C₆H₅CHO with O₂⁺ results in M⁺ and (M-H)⁺ as the only observed fragment (Španěl et al., 1997). The parent cation, and at least one fragmentation product, are observed for the reactions of ketones with O₂⁺ in SIFT-MS. As the ionization energies of ketones are usually low, exothermic charge transfer followed by multiple fragmentation processes is

TABLE 8 Ketones discussed in this review

Name/molecular formula	Method	reagent ion	Literature
C ₃ H ₆ O acetone	SIFT-MS PTR+SRI-MS	NO ⁺ O ₂ ⁺	Smith et al. (2019); Španěl and Smith (1996a); Wyche et al. (2005); Koss et al. (2016)
C ₄ H ₆ O butenone	PTR+SRI-MS	NO ⁺	Wyche et al. (2005)
C ₄ H ₆ O ₂ 2,3-butanedione	SIFT-MS	NO ⁺ O ₂ ⁺	Španěl et al. (1997)
C ₄ H ₈ O 2-butanone	SIFT-MS PTR+SRI-MS	NO ⁺ O ₂ ⁺	Smith et al. (2019); Španěl et al. (1997); Koss et al. (2016); Wyche et al. (2005)
C ₅ H ₈ O 3-methyl-3-buten-2-one	SIFT-MS	NO ⁺ O ₂ ⁺	Smith et al. (2019)
C ₅ H ₈ O ₂ 2,3-pentanedione	SIFT-MS	NO ⁺ O ₂ ⁺	Smith et al. (2019)
C ₅ H ₁₀ O 3-methyl-2-butanone	SIFT-MS	NO ⁺ O ₂ ⁺	Smith et al. (2019)
C ₅ H ₁₀ O 2-pentanone	SIFT-MS PTR+SRI-MS	NO ⁺ O ₂ ⁺	Smith et al. (2019); Španěl et al. (1997); Koss et al. (2016)
C ₅ H ₁₀ O 3-pentanone	SIFT-MS PTR+SRI-MS	NO ⁺ O ₂ ⁺	Španěl et al. (1997); Koss et al. (2016)
C ₆ H ₄ O ₂ 1,4-benzoquinone	SIFT-MS	NO ⁺ O ₂ ⁺	Smith et al. (2019), Wang et al. (2004)
C ₆ H ₁₀ O cyclohexanone	SIFT-MS	NO ⁺ O ₂ ⁺	Smith et al. (2019), Wang et al. (2004)
C ₆ H ₁₀ O 3-methyl-3-penten-2-one	SIFT-MS	NO ⁺ O ₂ ⁺	Smith et al. (2019)
C ₆ H ₁₀ O 4-methyl-3-penten-2-one	SIFT-MS	NO ⁺ O ₂ ⁺	Smith et al. (2019)
C ₆ H ₁₂ O 3-methyl-2-pentanone	SIFT-MS	NO ⁺ O ₂ ⁺	Smith et al. (2019)
C ₆ H ₁₂ O 4-methyl-2-pentanone	SIFT-MS	NO ⁺ O ₂ ⁺	Smith et al. (2019); Wang et al. (2004)
C ₆ H ₁₂ O 2-hexanone	SIFT-MS PTR+SRI-MS	NO ⁺ O ₂ ⁺	Smith et al. (2019); Španěl et al. (1997); Wang et al. (2004), Wyche et al. (2005)
C ₆ H ₁₂ O 3-hexanone	SIFT-MS PTR+SRI-MS	NO ⁺ O ₂ ⁺	Smith et al. (2019); Španěl et al. (1997); Wyche et al. (2005)
C ₆ H ₁₂ O ₂ 2,3-hexandione	SIFT-MS	NO ⁺ O ₂ ⁺	Smith et al. (2019); Španěl et al. (1997)
C ₇ H ₁₄ O 2-heptanone	SIFT-MS	NO ⁺ O ₂ ⁺	Smith et al. (2019)
C ₇ H ₁₄ O 3-heptanone	SIFT-MS	NO ⁺ O ₂ ⁺	Smith et al. (2019)
C ₈ H ₈ O 1-phenylethanone	SIFT-MS	NO ⁺ O ₂ ⁺	Smith et al. (2019); Španěl et al. (1997)
C ₈ H ₁₄ O 6-methyl-5-hepten-2-one	SIFT-MS	NO ⁺ O ₂ ⁺	Amelynck et al. (2005)

TABLE 8 (Continued)

Name/molecular formula	Method	reagent ion	Literature
C ₈ H ₁₆ O 3-octanone	SIFT-MS	NO ⁺ O ₂ ⁺	Smith et al. (2019)
C ₉ H ₁₈ O 2-nonanone	SIFT-MS	NO ⁺ O ₂ ⁺	Smith et al. (2019)
C ₁₀ H ₁₆ O camphor	SIFT-MS	NO ⁺ O ₂ ⁺	Amelynck et al. (2005)
C ₁₀ H ₁₈ O menthone	SIFT-MS	NO ⁺ O ₂ ⁺	Španěl et al. (1997)
C ₁₀ H ₂₀ O decanone	CI-MS* SIFT-MS	NO ⁺ O ₂ ⁺	Hearn and Smith (2004)*; Smith et al. (2019)

Note: If for a certain compound literature concerning both SIFT-MS and PTR+SRI-MS are given, references arising from PTR+SRI-MS are highlighted in bold. In case there is no literature given regarding SIFT-MS or PTR+SRI-MS, reactions in Chemical Ionization Mass Spectrometry (CI-MS) are also mentioned here and marked with *.

unavoidable (Španěl et al., 1997). For example, the reaction with acetone results in the parent cation [H₃CCOCH₃]⁺⁺ and the fragment ion [H₃CCO]⁺ in a 60/40 ratio (Smith et al., 2001; Španěl & Smith, 1996). However, this ratio also depends on the applied reduced electric field strength E/N, because at low energies more M⁺⁺ is observed (Spesvyi et al., 2017). Furthermore, with increasing atomicity of the ketones, the number of observed fragment ions increases accordingly, making the spectra more complex (Amelynck et al., 2005; Španěl et al., 1997; Wang et al., 2004). Using PTR+SRI-MS instead of SIFT-MS, fragmentation increases for aldehydes and ketones (Jordan, Haidacher, Hanel, Hartungen, Herbig, et al., 2009; Sulzer et al., 2012). In addition, these processes show a high sensitivity towards humidity (Wyche et al., 2005). For example, contamination with water opens protonation as an additional reaction pathway, which results in the elimination of H₂O, as shown for 1-hexanal by Wyche et al. (2005).

Compared to NO⁺ and O₂⁺, H₃O⁺ is ideal as a reagent ion for the detection of ketones because, in most of the cases, only the signal of the protonated molecule (MH)⁺ is observed (Španěl et al., 1997; Wyche et al., 2005). However, this is not observed for aldehydes. Instead, reactions of H₃O⁺ and C₄-aldehydes or larger homologues show a similar behavior to alcohols after protonation, leading to an elimination of H₂O⁺, and resulting in the detection of a carbohydrate product ion (MH-H₂O)⁺. Therefore, and due to its extent of lower fragmentation as compared to ionization with O₂⁺, NO⁺ is strongly recommended as a reactant for the identification of (aliphatic) aldehydes in both, SIFT-MS and PTR+SRI-MS (Amelynck et al., 2005; Španěl et al., 1997; Wyche et al., 2005).

2.5 | Reactions with carboxylic acids, carboxylic esters, and ethers

Carboxylic acids react via association or hydroxide transfer with NO⁺ in SIFT-MS (Španěl & Smith, 1998d) (Table 9). As already observed for aldehydes, the simplest carboxylic acid, formic acid HCOOH shows no reaction with NO⁺ as a reagent ion. This is consistent with theoretical calculations. The hydroxide transfer is endothermic (138 kJ mol⁻¹), and no bimolecular exothermic reaction channel is available (Španěl & Smith, 1998d). With hydroxide transfer still being endothermic (21 kJ mol⁻¹), the only compound for the reaction with acetic acid H₃CCOOH is the association product (H₃CCOOHNO)⁺. Hydroxide transfer takes place with propionic acid C₂H₅COOH for the first time, leading to 30% (C₂H₅CO)⁺, whereas 70% adduct (C₂H₅COOHNO)⁺ is detected. Extending the hydrocarbon chains and/or increasing the number of hydrocarbon substituents at the α-position leads to hydroxide transfer as the major pathway. For example (C₃H₇CO)⁺ arises with about 80% out of *iso*-butyric acid C₃H₇COOH, whereas only 50% of this fragment is observed for *n*-butyric acid. Interestingly, this is not the case for the unsaturated acrylic acid C₂H₃COOH, whereby the transfer of OH⁻ is only a minor pathway. In contrast to these results, Hearn et al. (Hearn & Smith, 2004) found no evidence of a OH⁻ loss for oleic acid C₁₇H₃₃COOH or linoleic acid C₁₇H₃₁COOH with NO⁺ in an aerosol CI-MS. Instead, they observed charge transfer, hydride transfer association, and H₂O loss for oleic acid. Association is the main reaction channel in a PTR+SRI-MS using a low reduced electric field strength, for example, 48 Td as was shown by Romano and Hanna (2018). Furthermore, association is the sole reaction with the cyclic

TABLE 9 Carboxylic acids, carboxylic esters and ethers discussed in this review

Name/molecular formula	Method	reagent ion	Literature
HCOOH formic acid	SIFT-MS	NO ⁺ O ₂ ⁺	Španěl and Smith (1998d)
H ₃ CCOOH acetic acid	SIFT-MS	NO ⁺ O ₂ ⁺	Španěl and Smith (1998d)
C ₂ H ₃ COOH acrylic acid	SIFT-MS	NO ⁺ O ₂ ⁺	Španěl and Smith (1998d)
C ₂ H ₄ OHCOOH lactic acid	SIFT-MS	NO ⁺ O ₂ ⁺	Španěl and Smith (1998d)
C ₂ H ₅ COOH propionic acid	SIFT-MS	NO ⁺ O ₂ ⁺	Španěl and Smith (1998d)
C ₃ H ₇ COOH <i>n</i> -butyric acid	SIFT-MS PTR+SRI-MS	NO ⁺ O ₂ ⁺	Španěl and Smith (1998d); Romano and Hanna (2018)
C ₃ H ₇ COOH <i>iso</i> -butyric acid	SIFT-MS	NO ⁺ O ₂ ⁺	Španěl and Smith (1998d)
C ₄ H ₉ COOH valeric acid	SIFT-MS PTR+SRI-MS	NO ⁺ O ₂ ⁺	Španěl and Smith (1998d); Romano and Hanna (2018)
C ₄ H ₉ COOH trimethylacetic acid	SIFT-MS	NO ⁺ O ₂ ⁺	Španěl and Smith (1998d)
C ₅ H ₁₁ COOH hexanoic acid	PTR+SRI-MS	NO ⁺ O ₂ ⁺	Romano and Hanna (2018)
C ₁₈ H ₃₂ O ₂ linoleic acid	CI-MS*	NO ⁺	Hearn and Smith (2004)*
C ₁₈ H ₃₄ O ₂ oleic acid	CI-MS*	NO ⁺	Hearn and Smith (2004)*
HCOOCH ₃ methyl formate	SIFT-MS	NO ⁺ O ₂ ⁺	Španěl and Smith (1998d)
HCOOC ₂ H ₅ ethyl formate	SIFT-MS	NO ⁺ O ₂ ⁺	Španěl and Smith (1998d)
CH ₃ COOCH ₃ methyl acetate	SIFT-MS	NO ⁺ O ₂ ⁺	Španěl and Smith (1998d)
CH ₃ COOC ₂ H ₅ ethyl acetate	SIFT-MS	NO ⁺ O ₂ ⁺	Španěl and Smith (1998d)
C ₂ H ₅ COOCH ₃ methyl propionate	SIFT-MS	NO ⁺ O ₂ ⁺	Španěl and Smith (1998d)
C ₂ H ₅ COOC ₂ H ₅ ethyl propionate	SIFT-MS	NO ⁺ O ₂ ⁺	Španěl and Smith (1998d)
C ₃ H ₇ COOCH ₃ methyl butyrate	SIFT-MS	NO ⁺ O ₂ ⁺	Španěl and Smith (1998d)
C ₆ H ₅ COOCH ₃ methyl benzoate	SIFT-MS	NO ⁺ O ₂ ⁺	Španěl and Smith (1998d)
C ₈ H ₁₄ O ₂ <i>cis</i> -3-hexenyl acetate	SIFT-MS	NO ⁺ O ₂ ⁺	Amelynck et al. (2005)
C ₃ H ₆ O ₂ 1,3-dioxalane	PTR+SRI-MS	NO ⁺	Mochalski et al. (2015)
C ₄ H ₄ O Furan	PTR+SRI-MS	NO ⁺	Mochalski et al. (2015)

TABLE 9 (Continued)

Name/molecular formula	Method	reagent ion	Literature
C ₄ H ₆ O 2,3-dihydrofuran	PTR+SRI-MS	NO ⁺	Mochalski et al. (2015)
C ₄ H ₆ O ₂ γ-butyrolactone	PTR+SRI-MS	NO ⁺	Mochalski et al. (2015)
C ₄ H ₈ O tetrahydrofuran	SIFT-MS	NO ⁺ O ₂ ⁺	Španěl and Smith (1998e)
C ₄ H ₈ O ₂ 2-methyl-1,3-dioxalane	PTR+SRI-MS	NO ⁺	Mochalski et al. (2015)
C ₄ H ₁₀ O diethylether	SIFT-MS	NO ⁺ O ₂ ⁺	Španěl and Smith (1998e)
C ₄ H ₁₀ O ₂ ethylene glycol dimethyl ether	SIFT-MS	NO ⁺ O ₂ ⁺	Španěl and Smith (1998e)
C ₅ H ₆ O 2-methylfuran	PTR+SRI-MS	NO ⁺	Mochalski et al. (2015)
C ₅ H ₆ O 3-methylfuran	PTR+SRI-MS	NO ⁺	Mochalski et al. (2015)
C ₅ H ₁₀ O allyl ethyl ether	SIFT-MS	NO ⁺ O ₂ ⁺	Španěl and Smith (1998e)
C ₅ H ₁₂ O butyl methyl ether	SIFT-MS	NO ⁺ O ₂ ⁺	Španěl and Smith (1998e)
C ₆ H ₈ O 2,5-dimethylfuran	PTR+SRI-MS	NO ⁺	Mochalski et al. (2015)
C ₆ H ₁₄ O tertiary pentyl methyl ether	SIFT-MS	NO ⁺ O ₂ ⁺	Španěl and Smith (1998e)
C ₆ H ₁₄ O butyl methyl ether	SIFT-MS	NO ⁺ O ₂ ⁺	Španěl and Smith (1998e)
C ₆ H ₁₄ O dipropyl ether	SIFT-MS	NO ⁺ O ₂ ⁺	Španěl and Smith (1998e)
C ₆ H ₁₄ O diisopropyl ether	SIFT-MS	NO ⁺ O ₂ ⁺	Španěl and Smith (1998e)
C ₇ H ₈ O anisole	SIFT-MS	NO ⁺ O ₂ ⁺	Španěl and Smith (1998e)
C ₉ H ₁₄ O 2-pentylfuran	PTR+SRI-MS	NO ⁺	Mochalski et al. (2015)
C ₁₀ H ₁₈ O 1,8-cineole	SIFT-MS	NO ⁺ O ₂ ⁺	Amelynck et al. (2005)

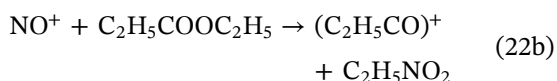
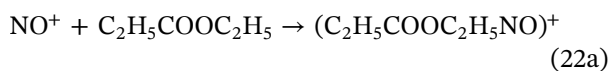
Note: If for a certain compound literature concerning both SIFT-MS and PTR+SRI-MS are given, references arising from PTR+SRI-MS are highlighted in bold. In case there is no literature given regarding SIFT-MS or PTR+SRI-MS, reactions in Chemical Ionization Mass Spectrometry (CI-MS) are also mentioned here and marked with *.

γ-butyrolactone C₄H₆O₂ at 110 Td, either in dry or humid (4.9% absolute humidity) air (Mochalski et al., 2015). These results once more emphasize the parallels between SIFT-MS and PTR+SRI-MS.

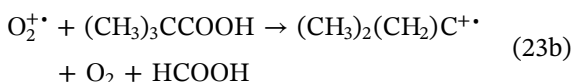
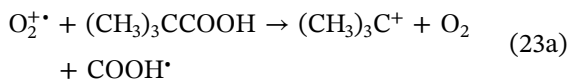
Besides association, which is the major pathway for lighter carboxylic esters in SIFT-MS with NO⁺, an additional reaction channel is observed (Španěl & Smith, 1998d).

Resulting in CH₃CO⁺ and CH₃NO₂, a transfer of CH₃O⁻ can be assumed. The involvement of a formal methoxide ion transfer is inferred by the thermochemical data, showing only a slight endothermicity, but explaining the low percentage (20%) observed (Lias et al., 1988). In addition, this fragmentation process is not limited to methyl-substituted esters, as an ethoxide transfer is observed for

ethylpropionate $\text{C}_2\text{H}_5\text{COOC}_2\text{H}_5$ in about 40% of $\text{C}_2\text{H}_5\text{CO}^+$ and $\text{C}_2\text{H}_5\text{NO}_2$ (Equation 22b).

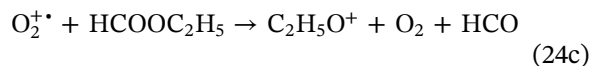
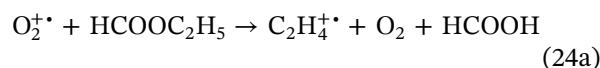


The alkoxide ion transfers become more exothermic with increasing alkyl chain length, thereby making ion transfer progressively more the preferred reaction pathway as chain length increases (Španěl & Smith, 1998d). Due to a lower ionization energy compared to $\text{O}_2^{+\bullet}$, charge transfer is the main, if not the only, reaction channel for carboxylic acids, and usually followed by fragmentation processes (Španěl & Smith, 1998d). However, the parent cation M^+ is not necessarily the detected main product. Formic acid HCOOH reacts with $\text{O}_2^{+\bullet}$ to either $(\text{H}_2\text{CO}_2)^+$ or $(\text{HCO}_2)^+$ in SIFT-MS. The former, which is the charge transfer product, is obtained in about 10% yield. The latter is built by dissociative charge transfer, which formally leads to the elimination of a free hydrogen atom in this case, or by hydride abstraction, as it cannot be ruled out. Hydride abstraction, which results in the formation of HO_2 , is usually observed in NO^+ measurements. However, it is not possible to detect neutral products with this analytical technique. Further investigations will be needed to answer this question. In case of carboxylic acids containing a secondary or a tertiary C-atom in α -position, the elimination of the neutral radical „COOH“ is observed (Equation 23) (Španěl & Smith, 1998d). Stabilized by positive inductive effects, this reaction channel is especially favored if it induces the formation of a tertiary carbocation, for example, for trimethylacetic acid $(\text{CH}_3)_3\text{CCOOH}$, whereby the cation is makes up about 90% of the product distribution (Equation 23a).



Dissociative charge transfer is also the main reaction channel for carboxylic acids in PTR+SRI-MS. The amount of fragmentation, which occurs after a successful charge transfer, is strongly affected by the choice of the reduced electric field strength, E/N. For example, using an E/N of 132 Td, which is in the standard range, no parent ion M^+ was detected for fatty acids (Romano & Hanna, 2018). Similar to organic acids, esters react via dissociative charge transfer with $\text{O}_2^{+\bullet}$ in SIFT-MS. Even if

a break in the C-O-C-bond is often observed resulting in $(\text{RCO})^+$ being part of the fragmentation spectrum, it is not possible to identify a clear overall trend in the fragmentation products. However, there is one special feature shown by Španěl and Smith (1998d), who investigated a series of different carboxylic esters in SIFT-MS. The dissociative charge transfer of ethyl formate HCOOC_2H_5 results in C_2H_4^+ making up over 90% of the product distribution (Equation 24a), with M^+ (Equation 24b) and $(\text{C}_2\text{H}_5\text{O})^+$ (Equation 24c) as minor side products. It is remarkable that hydrocarbon ions are the main products of this reaction, given that they form in of a reaction with $\text{O}_2^{+\bullet}$, which only happens occasionally.



Anisol $\text{C}_7\text{H}_8\text{O}$ is the only ether having charge transfer as main reaction channel with NO^+ in SIFT-MS (Španěl & Smith, 1998e). Most of the investigated compounds react via hydride transfer, as already observed for alcohols and aldehydes. The isomeric substances buthyl ethyl ether, dipropyl ether and diisopropyl ether, $\text{C}_6\text{H}_{13}\text{O}$, show $(\text{M-H})^+$ as the major products. For the latter ether, other side products resulting from alkyl transfer ($\text{R} = \text{CH}_3, \text{C}_3\text{H}_7$) are observed, giving the opportunity to distinguish between these compounds. Furan and several derivatives were investigated by Mochalski et al. (2015), showing charge transfer as a major channel in PTR+SRI-MS. Only two heterocycles, 2,3-dihydrofuran $\text{C}_4\text{H}_6\text{O}$ and 2-pentylfuran $\text{C}_9\text{H}_{14}\text{O}$, perform partial fragmentation, depending on the applied E/N. Anisol again exhibits special behavior with $\text{O}_2^{+\bullet}$ in SIFT-MS, as it shows no fragmentation after a successful charge transfer, which usually takes place in this class of compounds. However, even if the parent ion M^+ is mostly observed, there is again no clear trend in the fragmentation processes of ethers (Španěl & Smith, 1998e).

Besides small amounts of $(\text{MH-H}_2\text{O})^+$, mainly the protonated molecule ion is formed via the reaction of carboxylic acids and esters with H_3O^+ making H_3O^+ an excellent choice for the qualitative analysis of these kinds of compounds in SIFT-MS (Španěl & Smith, 1998e). Regarding PTR+SRI-MS a similar tendency is observed (Romano & Hanna, 2018). However, considering the analysis of ethers, reactions with H_3O^+ result in a larger variety of product ions compared to the reactions with

TABLE 10 Nitrogen containing species discussed in this review

Name/molecular formula	Method	reagent ion	Literature
C ₂ H ₃ N acetonitrile	SIFT-MS PTR+SRI-MS	NO ⁺ O ₂ ⁺	Španěl and Smith (1998a); Koss et al. (2016)
C ₇ H ₅ N Benzonitrile	SIFT-MS	NO ⁺ O ₂ ⁺	Španěl and Smith (1998a)
NH ₃ ammonia	SIFT-MS PTR+SRI-MS	NO ⁺ O ₂ ⁺	Smith et al. (2001); Španěl and Smith (1998a); Norman et al. (2007)
C ₂ H ₇ N dimethylamine	SIFT-MS	NO ⁺ O ₂ ⁺	Smith et al. (2001)
C ₃ H ₉ N Trimethylamine	SIFT-MS	NO ⁺ O ₂ ⁺	Španěl and Smith (1998a)
C ₃ H ₉ N Methylethylamine	SIFT-MS	NO ⁺ O ₂ ⁺	Španěl and Smith (1998a)
C ₃ H ₉ N Propylamine	SIFT-MS	NO ⁺ O ₂ ⁺	Španěl and Smith (1998a)
C ₃ H ₉ N Isopropylamine	SIFT-MS	NO ⁺ O ₂ ⁺	Španěl and Smith (1998a)
C ₄ H ₁₁ N Diethylamine	SIFT-MS	NO ⁺ O ₂ ⁺	Španěl and Smith (1998a)
C ₄ H ₁₁ N 1-Butylamine	SIFT-MS	NO ⁺ O ₂ ⁺	Španěl and Smith (1998a)
C ₅ H ₁₃ N 1-Pentylamine	SIFT-MS	NO ⁺ O ₂ ⁺	(Španěl and Smith 1998a, 1999c)
C ₅ H ₁₃ N 2-methylbutylamine	SIFT-MS	NO ⁺ O ₂ ⁺	Španěl and Smith (1999c)
C ₅ H ₁₃ N 3-methylbutylamine	SIFT-MS	NO ⁺ O ₂ ⁺	Španěl and Smith (1999c)
C ₅ H ₁₃ N 2-pentylamine	SIFT-MS	NO ⁺ O ₂ ⁺	Španěl and Smith (1999c)
C ₅ H ₁₃ N 3-methyl-2-butylamine	SIFT-MS	NO ⁺ O ₂ ⁺	Španěl and Smith (1999c)
C ₅ H ₁₃ N N-methylbutylamine	SIFT-MS	NO ⁺ O ₂ ⁺	Španěl and Smith (1999c)
C ₅ H ₁₃ N N-ethyl-2-propylamine	SIFT-MS	NO ⁺ O ₂ ⁺	Španěl and Smith (1999c)
C ₅ H ₁₃ N N,N-diethylmethylamine	SIFT-MS	NO ⁺ O ₂ ⁺	Španěl and Smith (1999c)
C ₅ H ₁₃ N N,N-dimethyl-2-propylamine	SIFT-MS	NO ⁺ O ₂ ⁺	Španěl and Smith (1999c)
C ₆ H ₇ N Aniline	SIFT-MS	NO ⁺ O ₂ ⁺	Španěl and Smith (1999a)
C ₆ H ₁₅ N Triethylamine	SIFT-MS	NO ⁺ O ₂ ⁺	Španěl and Smith (1999a)
CH ₃ NO ₂ nitromethane	SIFT-MS	NO ⁺ O ₂ ⁺	Dryahina et al. (2004)

(Continues)

TABLE 10 (Continued)

Name/molecular formula	Method	reagent ion	Literature
C ₂ H ₅ NO ₂ nitroethane	SIFT-MS	NO ⁺ O ₂ ⁺	Dryahina et al. (2004)
C ₃ H ₆ N ₆ O ₆ cyclotrimethylenetrinitramine	PTR+SRI-MS	NO ⁺ O ₂ ⁺	Sulzer et al. (2013)
C ₃ H ₇ NO ₂ 1-nitropropane	SIFT-MS	NO ⁺ O ₂ ⁺	Dryahina et al. (2004)
C ₃ H ₇ NO ₂ 2-nitropropane	SIFT-MS	NO ⁺ O ₂ ⁺	Dryahina et al. (2004)
C ₄ H ₉ NO ₂ 1-nitrobutane	SIFT-MS	NO ⁺ O ₂ ⁺	Dryahina et al. (2004)
C ₄ H ₉ NO ₂ 2-methyl-2-nitropropane	SIFT-MS	NO ⁺ O ₂ ⁺	Dryahina et al. (2004)
C ₅ H ₈ N ₄ O ₁₂ pentaerythritol tetranitrate	PTR+SRI-MS	NO ⁺ O ₂ ⁺	Sulzer et al. (2013)
C ₆ H ₃ N ₃ O ₆ 1,3,5-trinitrobenzene	PTR+SRI-MS	NO ⁺ O ₂ ⁺	Sulzer et al. (2013)
C ₆ H ₃ N ₃ O ₇ 2,4,6-trinitrophenol	PTR+SRI-MS	NO ⁺ O ₂ ⁺	Sulzer et al. (2013)
C ₇ H ₅ N ₃ O ₆ 2,4,6-trinitrotoluene	PTR+SRI-MS	NO ⁺ O ₂ ⁺	Sulzer et al. (2013)
C ₄ H ₄ N ₂ pyrimidine	PTR+SRI-MS	NO ⁺	Mochalski et al. (2015)
C ₄ H ₅ N pyrrole	SIFT-MS PTR+SRI-MS	NO ⁺ O ₂ ⁺	Španěl and Smith (1998a); Mochalski et al. (2015)
C ₅ H ₅ N pyridene	SIFT-MS PTR+SRI-MS	NO ⁺ O ₂ ⁺	Španěl and Smith (1998a); Mochalski et al. (2015)
C ₅ H ₆ N ₂ 4-methylpyrimidine	PTR+SRI-MS	NO ⁺	Mochalski et al. (2015)
C ₅ H ₇ N 1-methylpyrrole	PTR+SRI-MS	NO ⁺	Mochalski et al. (2015)
C ₇ H ₉ N 2,6-dimethylpyridine	PTR+SRI-MS	NO ⁺	Mochalski et al. (2015)

Note: If for a certain compound literature concerning both SIFT-MS and PTR+SRI-MS are given, references arising from PTR+SRI-MS are highlighted in bold. In case there is no literature given regarding SIFT-MS or PTR+SRI-MS, reactions in Chemical Ionization Mass Spectrometry (CI-MS) are also mentioned here and marked with *.

NO⁺, making NO⁺ a better choice for this class of compounds in SIFT-MS (Španěl & Smith, 1998e).

2.6 | Reactions with nitrogen containing species

Besides oxygen-containing substances, compounds including nitrogen are another important aspect in gas analysis as such molecules can have numerous undesirable effects on living beings and the environment

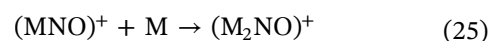
(Table 10). Therefore the investigation of both small inorganic, for example, HCN, NO_x, NH₃ and so on. as well as organic molecules, for example, acetonitrile, amines, heterocycles and so on are of high concern (Chai et al., 2019; Jürschik et al., 2010; Knighton et al., 2009; Moussa et al., 2016; Pugliese et al., 2019). Detailed investigations by Španěl and Smith (1998a, 1999c) showed that associative and dissociative charge transfer, as well as hydride abstraction are possible reactions for amines with NO⁺ in SIFT-MS (Table 11).

Smaller primary 1-amines (C₃-C₅) react via hydride abstraction from a carbon-atom as a major pathway, while primary (branched) amines, with NH₂ being on the second or third position, react mainly via charge transfer, usually followed by fragmentation (Španěl & Smith, 1998a). 1-pentylamine, C₅H₁₁NH₂, offers 65% (M-H)⁺, whereas the main product for 2-pentylamine and 3-methyl-2-butylamine is (C₂H₄NH₂)⁺, results from dissociative charge transfer (Španěl & Smith, 1999c). M⁺ is found to be a major product for the smaller dimethylamine, (CH₃)₂NH, methylethylamine, (C₂H₅)CH₃NH and diethylamine, (C₂H₅)₂NH (Španěl & Smith, 1998a). Again, fragmentation is observed regarding secondary amines with larger substituents, for example, N-ethyl-2-propylamine (Španěl & Smith, 1999c). The same is determined for tertiary amines, as the percentage of dissociative charge transfer increases by increasing substituent length (Španěl & Smith, 1999a). Contrary to NO⁺, where no successful reaction with ammonia NH₃ (IE 10.07 eV) occurs, charge transfer takes place using O₂⁺ as a reagent ion (Norman et al., 2007). Thereby, no formation of water-clusters in SIFT-MS was observed in PTR+SRI-MS in humid air, which can be attributed to the use of a drift tube. Nevertheless, the M⁺ signal decreases at standard operating conditions (*T* = 25°C, *E*/*N* = 132 Td) to about 80%. All reactions of alkyl-amines with O₂⁺ proceed via dissociative charge transfer in SIFT-MS. CH₄N⁺, presumably having an ammonium structure H₂C = NH₂⁺, appears often as fragment ion for primary amines (Španěl & Smith, 1998a). Additionally, the ions that result from the elimination of the largest radical also occur frequently. Due to the multiple fragmentation processes, it is straightforward to compare the mass spectra of the ionization with O₂⁺ in SIFT-MS with EI-MS (70 eV). In both methods, the major fragment ions, and therefore, the fragmentation processes are in principle the same. However, explained by the higher excess in energy in EI-MS, more minor fragmentation products are observed (Španěl & Smith, 1999c). In contrast, no fragmentation is observed for heteroaromatic compounds, neither for NO⁺ nor O₂⁺ ionization. The only reaction proceeding for pyrrole C₄H₅N is charge transfer, which is observed for both reagent ions in SIFT-MS and PTR+SRI-MS (Mochalski et al., 2015; Španěl & Smith, 1998a). The same is observed for pyridine C₅H₅N with O₂⁺. In contrast, the main reaction channel with NO⁺ in SIFT-MS is association (70%), whereas charge transfer is only a minor reaction channel. This behavior is explained by the slightly higher ionization energy of pyridine compared to NO⁺. Nevertheless, charge transfer can appear through a parallel intermolecular ion-molecule interaction, based on the phenomenon of „charge transfer complexing“, which was already

described above for ketones (Mochalski et al., 2015; Španěl & Smith, 1999a). A similar observation is made for 2,6-dimethylpyridine C₇H₉N, pyrimidine C₄H₄N₂, and 4-methylpyrimidine C₅H₆N₂, as all compounds feature ionization energies close to NO⁺. Changing the reduced electric field strength *E*/*N* in PTR+SRI-MS has again a major influence on the ratio between both reaction channels. For example, increasing *E*/*N* suppresses the adduct formation, whereas at 90 Td, 70% M⁺ are detected for 4-methylpyrimidine, it decreases to 25% at 130 Td.

Detailed investigations were made concerning acetonitrile CH₃CN, as it shows a lifetime of several months in the earth's atmosphere, and is an indicator for biomass burning (de Gouw, Warneke, et al., 2003; Dunne et al., 2012). In SIFT-MS, NO⁺ adduct formation is observed, as it is only reaction path of acetonitrile (IE 12.20 eV) (Gochel-Dupuis et al., 1992; Španěl & Smith, 1998a). In contrast, in PTR+SRI-MS mainly the charge transfer product M⁺ (87%) is detected (Blake et al., 2006). This is once more emphasizing the influence of the drift tube and the reduced electrical field strength (*E*/*N* = 165 Td), as the ionization energy of CH₃CN is nearly 3 eV higher compared to NO⁺. Still, (C₂H₂NNO)⁺ is reported as a minor product, revealing that that adduct formation is nevertheless possible. Also by reaction with O₂⁺ in PTR+SRI-MS, only charge transfer products and the parent ion (CH₃CN)⁺ are observed. Besides the endothermic charge transfer reaction, an association product was also documented in SIFT-MS (Španěl & Smith, 1998a). The formation of this adduct, (CH₃CNO₂)⁺, is explained by the similar ionization energies of acetonitrile and O₂⁺, presumably leading to a charge transfer complexing.

Nitroalkanes, for example, nitromethane CH₃NO₂, nitroethane C₂H₅NO₂, nitropropane C₃H₇NO₂ and so on, exhibit mainly adduct formation with NO⁺ in SIFT-MS (Dryahina et al., 2004). These ions show interesting reactivity as they associate with a parent molecule resulting in a NO⁺ bound dimer (Equation 25).



Other pathways are not observed for these molecules, as the ionization energy of nitroalkanes is higher than NO⁺, and hydride transfer is endothermic. However, 1-Nitrobutane C₄H₉NO₂ and its isomer, 2-methyl-2-nitropropane, show dissociative charge transfer resulting in the hydrocarbon ion C₄H₉⁺ and the neutral N₂O₃. Interestingly, this NO₂ abstraction is the only reaction channel for the branched nitroalkane, whereas it is solely a minor reaction channel (15%) for the linear compound. Investigations in PTR+SRI-MS reveal association as the only

TABLE 11 Reactions of selected nitrogen-containing compounds in SIFT-MS (Španěl & Smith, 1998a, 1999c)

Compound	Structure	NO ⁺	O ₂ ⁺
Ammonia		no reaction	NH ₃ ⁺ (100)
Propylamine		C ₃ H ₈ N ⁺ (75) C ₃ H ₉ N ⁺ (25)	CH ₄ N ⁺ (100)
iso-Propylamine		C ₃ H ₈ N ⁺ (45) C ₂ H ₆ N ⁺ (50) others (5)	C ₂ H ₆ N ⁺ (75) CH ₅ N ⁺ (10) C ₃ H ₈ N ⁺ (5) others (10)
1-Pentylamine		C ₅ H ₁₂ N ⁺ (65) C ₅ H ₁₃ N ⁺ (35)	CH ₄ N ⁺ (90) C ₅ H ₁₃ N ⁺ (5) C ₂ H ₇ N ⁺ (5)
2-Pentylamine		C ₂ H ₆ N ⁺ (65) C ₅ H ₁₂ N ⁺ (25) C ₅ H ₁₃ N ⁺ (10)	C ₂ H ₆ N ⁺ (95) C ₄ H ₁₀ N ⁺ (5)
Dimethylamine		C ₂ H ₇ N ⁺ (95) C ₂ H ₆ N ⁺ (5)	C ₂ H ₇ N ⁺ (70) C ₂ H ₆ N ⁺ (30)
N-ethyl-2-propylamine		C ₄ H ₁₀ N ⁺ (70) C ₅ H ₁₃ N ⁺ (30)	C ₄ H ₁₀ N ⁺ (90) C ₂ H ₆ N ⁺ (10)
Triethylamine		C ₆ H ₁₅ N ⁺ (90) C ₅ H ₁₂ N ⁺ (10)	C ₅ H ₁₂ N ⁺ (100)
Aniline		C ₆ H ₇ N ⁺ (100)	C ₆ H ₇ N ⁺ (100)
Pyridine		(C ₅ H ₅ NNO) ⁺ (70) C ₅ H ₅ N ⁺ (30)	C ₅ H ₅ N ⁺ (100)
Acetonitrile	CH ₃ CN	(CH ₃ CNNO) ⁺ (100)	CH ₃ CN ⁺ (CH ₃ CNO ₂) ⁺
Benzonitrile		(C ₆ H ₅ CNNO) ⁺ (100)	(C ₆ H ₅ CN) ⁺ (100)

reaction channel for NO⁺ with several explosive nitrocompounds (Agarwal et al., 2014; Sulzer et al., 2013). Even if explosives are relatively uncommon analytes, those examinations emphasize once again the importance of the right choice of the selected E/N concerning the measurement task, as the signal intensities drop significantly with increasing E/N.

Although the recombination energy of O₂⁺ (12.07 eV) is adequate for charge transfer reactions with the investigated explosives in PTR+SRI-MS, it is not observed in all cases. Cyclotrimethylenetrinitramine C₃H₆N₆O₆ and pentaerythritol tetranitrate C₅H₈N₄O₁₂ offer no reactivity, contrary to 2,4,6-trinitrotoluene C₇H₅N₃O₆, 1,3,5-trinitrobenzene C₆H₃N₃O₆ and picric acid C₆H₃N₃O₇. All of these molecules exhibit ionization

energies below O₂⁺, but only the aromatic substances react via (dissociative) charge transfer (Agarwal et al., 2014; Sulzer et al., 2013). Not to be ignored are the results in SIFT-MS given by Dryahina et al. (Dryahina et al., 2004), as only nitromethane CH₃NO₂ offers a parent ion signal. For all other analyzed nitroalkanes (C₂–C₄), a complete NO₂ elimination occurs, resulting in one single signal for the corresponding carbohydrate cation C_xH_{2x+1}⁺. As neither fragmentation patterns nor parent ion signals are detectable, an assignment of these substances in a complex mixture seems not feasible. Although these carbohydrate cations undergo a variety of secondary reactions, an identification of presumed nitroalkanes or a qualitative validation of a single compound is reasonable (Dryahina et al., 2004).

For most of the investigated nitrogen compounds, H_3O^+ is also a good choice as a reagent ion regarding qualitative and partially quantitative analysis, although some fragmentation processes occur. Reactions with primary amines show partial dissociation of NH_4^+ after protonation or an H_2 elimination for secondary and tertiary amines (Španěl & Smith, 1998a, 1999c). In case of 2-nitropropane $\text{C}_3\text{H}_7\text{NO}_2$ even HNO elimination leading to $\text{C}_3\text{H}_7\text{O}^+$ is observed (Dryahina et al., 2004). Nevertheless, these are only minor exceptions, as MH^+ gives the main signal for most of the investigated compounds in SIFT-MS. Therefore, additional measurements with NO^+ and O_2^{+*} are a good support for H_3O^+ , but not a necessity in this case.

2.7 | Reactions with organosulfur and organoselenium compounds

Determining organosulfur is not only of high concern for industrial processes, for example, in methanol synthesis, where sulfur acts as catalyst poison (Schittkowski et al., 2018), but also in medicine, as volatile sulfur and selenium compounds can become toxic in higher concentrations (Haick et al., 2014; Sovova et al., 2012) (Table 12). H_2S (IE 10.45 eV) (Walters & Blais, 1984) and H_2Se (IE 9.89 eV) (Sovova et al., 2012) can neither be measured by NO^+ nor O_2^{+*} in SIFT-MS. With O_2^{+*} having enough energy required, the resulting H_2S^+ and H_2Se^+ , respectively, reacts immediately with H_2O to form H_3O^+ (Pysanenko et al., 2008; Sovova et al., 2012). Therefore, a measurement in SIFT-MS is only possible with H_3O^+ . In contrast, besides H_3O^+ O_2^{+*} can most likely be used as a reagent for both H_2S and H_2Se , in PTR+SRI-MS. First, this technique offers a much higher reagent ion selectivity compared to SIFT-MS; and second, it is possible to measure under complete dry conditions in PTR+SRI-MS with O_2^{+*} as a reagent ion, whereas the O_2^{+*} in SIFT-MS is selected from a wet air plasma produced via microwave discharge (Smith & Španěl, 2005). Regarding organosulfur compounds, the reaction of methanthiol CH_3SH with NO^+ is relatively slow compared to O_2^{+*} . Furthermore, the signal of the major product CH_3SH^+ overlaps with the signal of the adduct ion $\text{NO}^+\text{H}_2\text{O}^+$, which is formed in humid samples. Therefore, NO^+ is unsuitable for the analysis of CH_3SH in SIFT-MS for humid samples (Pysanenko et al., 2008). However, a high-resolution PTR+SRI-MS can separate both signals making a proper detection possible. Only charge transfer is observed for sulfides R_2S and disulfides R_2S_2 ($\text{R} = \text{CH}_3$, C_3H_5) with NO^+ in SIFT-MS, whereas PTR+SRI-MS shows less selectivity based on several fragmentation

processes (Mochalski et al., 2014b; Španěl & Smith, 1998c). In most cases, M^+ is still the main signal (Table 13) at both, dry (a) and humid (b) conditions (AH 4.9%, $\text{E}/\text{N} = 130$), except for methyl propyl sulfide $\text{C}_4\text{H}_{10}\text{S}$, resulting in 20% (a)/25% (b) M^+ and $(\text{CH}_5\text{S})^+$ with 39% (a)/36% (b) as main products. In contrast, 85% (a)/87% (b) M^+ is detected for allyl methyl sulfide, and interestingly no attack of the double bond, leading to a stable cationic association product, was observed. This example suggests, even if longer alkyl chains results in higher fragmentation, dissociation of M^+ is hindered by unsaturated substituents, as proposed by Mochalski et al. (2014b). The major product for thiophene $\text{C}_4\text{H}_4\text{S}$ and its methyl-substituted derivatives in PTR+SRI-MS, whether at dry or humid conditions, is the charge transfer product M^+ (Table 13), which is in accordance to previously reported aromatic compounds (Mochalski et al., 2014b).

Selenides R_2Se and diselenides, R_2Se_2 , exemplifying the dimethyl-substituted compounds, react nearly quantitatively with NO^+ through a charge transfer reaction in both SIFT-MS and PTR+SRI-MS (Table 13) (Mochalski et al., 2014b; Sovova et al., 2012). Five of the six naturally existing isotopes of selenium are stable, which presents the possibility of clearly identifying those compounds by means of their isotopic patterns in the mass spectra (Figure 4), even in a complex sample.

NO^+ is not suitable for the analysis of carbon disulfide because the reaction is very slow, and leads to the adduct ion CS_2NO^+ (Pysanenko et al., 2008). In contrast, O_2^{+*} offers a fast charge transfer reaction with CS_2 . Still, determination of this trace compound with O_2^{+*} in SIFT-MS proves to be difficult because the signal occurring at $m/z = 76$ potentially overlaps with $[\text{CO}_2\text{O}_2]^+$, and additionally with $[\text{CH}_3\text{COCH}_3\text{H}_2\text{O}]^+$ in humid samples. CO_2O_2^+ results through a three-body reaction of CO_2 , O_2^{+*} and the carrier gas molecule He. $\text{CH}_3\text{COCH}_3\text{H}_2\text{O}^+$ is the adduct of the charge transfer product of $[\text{CH}_3\text{COCH}_3]$ with water. Both, carbon dioxide and acetone are usually present in a common sample, and water is, in most of the cases and at least in SIFT-MS, unavoidable. Additionally, depending on the sample the concentration of CS_2 is low compared to CO_2 and acetone, which are in a similar range, for example, for air samples (Pysanenko et al., 2008). However, PTR+SRI-MS might overcome this task as at higher E/N the formation of adducts like $[\text{CO}_2\text{O}_2]^+$ is suppressed and the higher mass resolution might separate the signals (Sulzer et al., 2014). Unfortunately, there are no investigations on this special case known in the literature.

CH_3SH^+ is, similar to its reaction with NO^+ , the major product of the reaction of CH_3SH with O_2^{+*} (Pysanenko et al., 2008). Even if the reaction is much faster compared to NO^+ , the signal of CH_3SH^+ overlaps

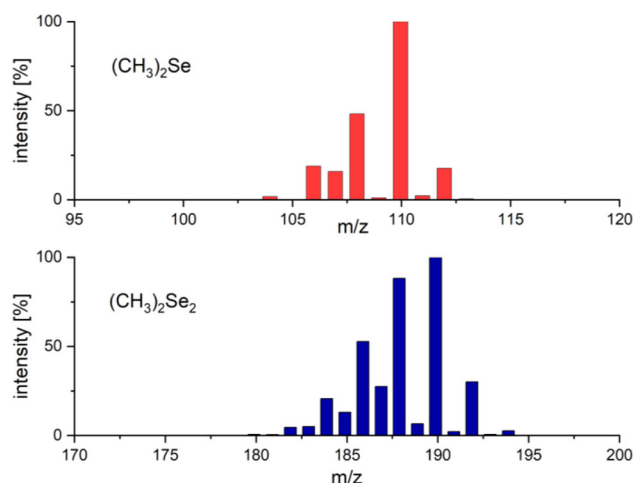
TABLE 12 Organosulfur and organoselenium compounds discussed in this review

Name/molecular formula	Method	Reagent ion	Literature
CS ₂ carbon disulfide	SIFT-MS	NO ⁺ O ₂ ⁺	Pysanenko et al. (2008); Španěl and Smith (1998c)
CH ₄ S methanethiol	SIFT-MS PTR+SRI-MS	NO ⁺ O ₂ ⁺	Pysanenko et al. (2008); Mochalski et al. (2014b)
C ₂ H ₆ S dimethyl sulfide	SIFT-MS PTR+SRI-MS	NO ⁺ O ₂ ⁺	Pysanenko et al. (2008); Španěl and Smith (1998c); Mochalski et al. (2014b)
C ₂ H ₆ S ₂ dimethyl disulfide	SIFT-MS PTR+SRI-MS	NO ⁺ O ₂ ⁺	Pysanenko et al. (2008); Španěl and Smith (1998c); Mochalski et al. (2014b)
C ₂ H ₆ S ethanthiol	SIFT-MS	NO ⁺ O ₂ ⁺	Španěl and Smith (1998c)
C ₃ H ₈ S ethyl methyl sulfide	PTR+SRI-MS	NO ⁺	Mochalski et al. (2014b)
C ₄ H ₄ S thiophene	PTR+SRI-MS	NO ⁺	Mochalski et al. (2014b)
C ₄ H ₈ S allyl methyl sulfide	PTR+SRI-MS	NO ⁺	Mochalski et al. (2014b)
C ₄ H ₁₀ S methyl propyl sulfide	PTR+SRI-MS	NO ⁺	Mochalski et al. (2014b)
C ₅ H ₆ S 2-methylthiophene	PTR+SRI-MS	NO ⁺	Mochalski et al. (2014b)
C ₅ H ₆ S 3-methylthiophene	PTR+SRI-MS	NO ⁺	Mochalski et al. (2014b)
C ₂ H ₄ OS thiolacetic acid	SIFT-MS	NO ⁺ O ₂ ⁺	Španěl and Smith (1998c)
C ₂ H ₆ OS dimethyl sulfoxide	PTR+SRI-MS	NO ⁺	Mochalski et al. (2014b)
C ₆ H ₈ OS methyl 5-methyl-2-furyl sulfide	PTR+SRI-MS	NO ⁺	Mochalski et al. (2014b)
C ₄ H ₅ NS allyl isothiocyanate	PTR+SRI-MS	NO ⁺	Mochalski et al. (2014b)
C ₄ H ₈ S ₂ 1,3 dithiane	SIFT-MS	NO ⁺ O ₂ ⁺	Španěl and Smith (1998c)
C ₆ H ₁₀ S ₂ diallyl disulfide	SIFT-MS	NO ⁺ O ₂ ⁺	Španěl and Smith (1998c)
C ₂ H ₆ S ₃ dimethyl trisulphide	PTR+SRI-MS	NO ⁺	Mochalski et al. (2014b)
CH ₄ Se methylselenol	SIFT-MS	NO ⁺ O ₂ ⁺	Sovova et al. (2012)
C ₂ H ₆ Se dimethyl selenide	SIFT-MS PTR+SRI-MS	NO ⁺ O ₂ ⁺	Sovova et al. (2012); Mochalski et al. (2014b)
C ₂ H ₆ Se ₂ dimethyl diselenide	SIFT-MS PTR+SRI-MS	NO ⁺ O ₂ ⁺	Sovova et al. (2012); Mochalski et al. (2014b)

Note: If for a certain compound literature concerning both SIFT-MS and PTR+SRI-MS are given, references arising from PTR+SRI-MS are highlighted in bold. In case there is no literature given regarding SIFT-MS or PTR+SRI-MS, reactions in Chemical Ionization Mass Spectrometry (CI-MS) are also mentioned here and marked with *.

TABLE 13 Ion distribution of selected organosulfur and organoselenium compounds in SIFT-MS and PTR+SRI-MS (Mochalski et al., 2014b, Pysanenko et al., 2008, Sovova et al., 2012, Španěl & Smith, 1998c)

Compound	Formula	SIFT-MS (NO ⁺)	PTR+SRI-MS (NO ⁺ , E/N 130 Td) (dry/AH 4.9%)
Carbon disulfide	CS ₂	CS ₂ NO ⁺	-
Methanethiol	CH ₃ SH	CH ₃ SH ⁺	CH ₃ SH ⁺ (82/82) CH ₃ SHNO ⁺ (>6/>8) CH ₃ S ⁺ (7/<5) CHS ⁺ (>4/>5)
Thiophene	C ₄ H ₄ S	-	C ₄ H ₄ S ⁺ (100/100)
2-Methylthiophene	C ₅ H ₆ S	-	C ₅ H ₆ S ⁺ (97/98) C ₅ H ₅ S ⁺ (<3/>2)
Dimethylsulphide	(CH ₃) ₂ S	(CH ₃) ₂ S ⁺ (100)	C ₂ H ₆ S ⁺ (91/94) CH ₃ S ⁺ (9/6)
Dimethyldisulphide	(CH ₃) ₂ S ₂	(CH ₃) ₂ S ₂ ⁺ (100)	C ₂ H ₆ S ₂ ⁺ (93/91) CH ₃ S ₂ ⁺ (<1/<1) C ₂ H ₆ S ⁺ (<7/>8)
Dimethylselenide	(CH ₃) ₂ Se	(CH ₃) ₂ Se (100)	C ₂ H ₆ Se ⁺ (99/99) CH ₃ Se ⁺ (>1/1)
Dimethyldiselenide	(CH ₃) ₂ Se ₂	(CH ₃) ₂ Se ₂ ⁺ (100)	C ₂ H ₆ Se ₂ ⁺ (99/99) CH ₃ Se ₂ ⁺ (<1/<1)

**FIGURE 4** Simulated isotopic patterns of (CH₃)₂Se and (CH₃)₂Se₂ according to (Patiny & Borel, 2013)

with the signal for NOH₂O⁺, making O₂⁺ unsuitable as NO⁺ impurities are always present with O₂⁺ as reagent ions in SIFT-MS and in PTR+SRI-MS. Therefore, the only way for a proper detection of CH₃SH in SIFT-MS is the usage of H₃O⁺ as a reagent ion, leading to CH₃SHH⁺. However, PTR+SRI-MS, as a high resolution device, can overcome this problem and separate the signals of CH₃SH⁺ and NOH₂O (Pysanenko et al., 2008).

Besides charge the transfer, hydride abstraction and association reaction pathways, ethanethiol C₂H₅SH offers

sulfhydryl transfer as a fourth reaction pathway with NO⁺ in SIFT-MS (Španěl & Smith, 1998c). Similar to the well investigated hydroxide transfer observed with alcohols, sulfhydryl transfer takes place in thiols. Thereby, the abstraction of the sulfhydryl anion SH⁻ is observed, resulting in HNOS (Equation 25).



M⁺ is also the main signal (around 50%) of ethanethiol C₂H₅SH and O₂⁺ in SIFT-MS, and the overall signal is completed with several fragmentation products. Concerning selenols and NO⁺ or O₂⁺ as reagent ions, there are no detailed investigations in either SIFT-MS nor PTR+SRI-MS. Therefore, only speculations derived on observations with organothiols can be made (Sovova et al., 2012).

As all investigated sulfur compounds can be qualitatively and quantitatively determined with H₃O⁺, except CS₂ due to its endothermic protonation (Pysanenko et al., 2008; Španěl & Smith, 1998c), the additional use of NO⁺ and O₂⁺ will provide little further insight into this compound class in SIFT-MS. However, further investigations using H₃O⁺ and O₂⁺ in PTR+SRI-MS are required to solve the special case for CS₂ as well as for COS, which are only poorly detectably using H₃O⁺ as the reagent ion, due to its low proton affinity (Hunter & Lias, 1998).

TABLE 14 Halocarbons discussed in this review

Name/molecular formula	Method	reagent ion	Literature
C ₂ F ₄ tetrafluoroethene	SIFT-MS	O ₂ ⁺	Jarvis et al. (2000)
C ₃ F ₆ hexafluoropropylene	SIFT-MS	O ₂ ⁺	Jarvis et al. (2000)
C ₄ F ₈ 2-octafluorobuthene	SIFT-MS	O ₂ ⁺	Jarvis et al. (2000)
C ₆ H ₅ F fluorobenzene	SIFT-MS	NO ⁺ O ₂ ⁺	Španěl and Smith (1999a)
C ₇ H ₇ F 2-fluorotoluene	SIFT-MS	NO ⁺ O ₂ ⁺	Španěl and Smith (1999a)
C ₇ H ₇ F 4-fluorotoluene	SIFT-MS	NO ⁺ O ₂ ⁺	Španěl and Smith (1999a)
CH ₃ Cl chloromethane	SIFT-MS	NO ⁺ O ₂ ⁺	Španěl and Smith (1999a)
CH ₂ Cl ₂ dichloromethane	SIFT-MS	NO ⁺ O ₂ ⁺	Španěl and Smith (1999b)
CHCl ₃ chloroform	SIFT-MS	NO ⁺ O ₂ ⁺	Španěl and Smith (1999b)
CCl ₄ tetrachloromethane	SIFT-MS	NO ⁺ O ₂ ⁺	Španěl and Smith (1999b)
C ₂ HCl ₃ trichloroethylene	SIFT-MS	NO ⁺ O ₂ ⁺	Španěl and Smith (1999b)
C ₂ Cl ₄ tetrachloroethylene	SIFT-MS	NO ⁺ O ₂ ⁺	Španěl and Smith (1999b)
C ₂ H ₆ Cl ₂ 1,2-dichloroethane	SIFT-MS	NO ⁺ O ₂ ⁺	Španěl and Smith (1999b)
C ₂ H ₆ Cl ₂ 1,1-dichloroethane	SIFT-MS	NO ⁺ O ₂ ⁺	Španěl and Smith (1999b)
C ₂ H ₃ Cl ₃ 1,1,1-trichloroethane	SIFT-MS	NO ⁺ O ₂ ⁺	Španěl and Smith (1999b)
C ₂ H ₂ Cl ₄ 1,1,2,2-tetrachloroethane	SIFT-MS	NO ⁺ O ₂ ⁺	Španěl and Smith (1999b)
C ₆ H ₅ Cl chlorobenzene	SIFT-MS PTR+SRI-MS	NO ⁺ O ₂ ⁺	Španěl and Smith (1999a); Jordan, Haidacher, Hanel, Hartungen, Herbig, et al. (2009)
C ₇ H ₇ Cl benzylchloride	SIFT-MS	NO ⁺ O ₂ ⁺	Španěl and Smith (1999a)
C ₇ H ₇ Cl 2-chlorotoluene	SIFT-MS	NO ⁺ O ₂ ⁺	Španěl and Smith (1999a)
C ₇ H ₇ Cl 4-chlorotoluene	SIFT-MS	NO ⁺ O ₂ ⁺	Španěl and Smith (1999a)
C ₆ H ₄ Cl ₂ dichlorobenzene	PTR+SRI-MS	NO ⁺ O ₂ ⁺	Jordan, Haidacher, Hanel, Hartungen, Herbig, et al. (2009)
C ₆ H ₃ Cl ₃ trichlorobenzene	PTR+SRI-MS	NO ⁺ O ₂ ⁺	Jordan, Haidacher, Hanel, Hartungen, Herbig, et al. (2009)

TABLE 14 (Continued)

Name/molecular formula	Method	reagent ion	Literature
C ₆ H ₅ Br bromobenzene	SIFT-MS	NO ⁺ O ₂ ⁺	Španěl and Smith (1999a)
C ₇ H ₇ Br benzylbromide	SIFT-MS	NO ⁺ O ₂ ⁺	Španěl and Smith (1999a)
C ₇ H ₇ Br 2-bromotoluene	SIFT-MS	NO ⁺ O ₂ ⁺	Španěl and Smith (1999a)
C ₇ H ₇ Br 4-bromotoluene	SIFT-MS	NO ⁺ O ₂ ⁺	Španěl and Smith (1999a)
C ₆ H ₅ I iodobenzene	SIFT-MS	NO ⁺ O ₂ ⁺	Španěl and Smith (1999a)
C ₇ H ₇ I 2-iodotoluene	SIFT-MS	NO ⁺ O ₂ ⁺	Španěl and Smith (1999a)
C ₇ H ₇ I 4-iodotoluene	SIFT-MS	NO ⁺ O ₂ ⁺	Španěl and Smith (1999a)

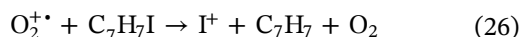
Note: If for a certain compound literature concerning both SIFT-MS and PTR+SRI-MS are given, references arising from PTR+SRI-MS are highlighted in bold. In case there is no literature given regarding SIFT-MS or PTR+SRI-MS, reactions in Chemical Ionization Mass Spectrometry (CI-MS) are also mentioned here and marked with *.

2.8 | Reactions with halocarbons

In general, perfluorocarbons exhibit a high ionization potential, explaining why they are lightly unreactive towards NO⁺ in SIFT-MS (Jarvis et al., 2000) (Table 14). For example, CF₄, C₂F₆ and C₃F₈, which are known to be strong greenhouse gases (Myhre et al., 2013), show even higher ionization potentials compared to O₂⁺. Nevertheless, unsaturated perfluorocarbons react with O₂⁺, mainly via non-dissociative charge transfer (Jarvis et al., 2000). Whereas M⁺ is exclusively formed with C₂F₄, slight branching is observed for C₃F₆ and C₄F₈, leading to the detection of the fragment cations [C₂F₄]⁺ and [C₃F₅]⁺. Almost all reactions of chlorinated hydrocarbons investigated in SIFT-MS with NO⁺ are association reactions based on a three-body reaction with carrier gas molecules (Španěl & Smith, 1999a, 1999b). Again, the previously mentioned charge transfer complexing plays a decisive role, for example, for CH₃Cl and C₂H₅Cl, as their ionization energies are much greater than NO⁺. Thus, the reaction, which would usually be inefficient and not occur, is only decelerated (Španěl & Smith, 1999a). Interestingly, 1,1,1-trichloroethane reacts completely abnormally by chloride ion abstraction, resulting in NOCl and [H₃CCCl₂]⁺. Based on the given thermochemical and kinetic data, the reaction must be quite exothermic as it proceeds rapidly. However, the reaction pathway remains unclear, as dissociative charge transfer is excluded due to the high ionization energy of H₃CCCl₃

(Španěl & Smith, 1999b). Dichloromethane CH₂Cl₂ and chloroform CHCl₃, both unreactive towards NO⁺, react via (dissociative) charge transfer with O₂⁺ in SIFT-MS leading to [CH₂Cl₂]⁺ and [CHCl₂]⁺, respectively. A chlorine loss resulting in [M-Cl]⁺ is also observed for tetrachloromethane CCl₄, 1,1-dichloroethane H₂ClCCH₂Cl and 1,1,1-trichloroethane Cl₃CCH₃. H₂ClCCH₂Cl and C₂H₅Cl eliminate mainly HCl arising the corresponding cation after a charge transfer. The chloroethylenes C₂Cl₄ and HClCCl₂ react solely either by association with NO⁺ or by charge transfer with O₂⁺. Similar to the lighter monochlorinated compounds, brominated as well as iodinated methane and ethane show adduct formation with NO⁺ in SIFT-MS (Španěl & Smith, 1999a). The reaction with O₂⁺ as the reagent ion leads either to M⁺ for mono-halogenated methanes or a mixture of mainly M⁺ and [M-X]⁺ (X = Br, I) for ethanes through charge transfer. The elimination of HX, as observed for C₂H₅Cl in SIFT-MS, could not be determined (Španěl & Smith, 1999a). Phenyl halides, C₆H₅X (X = Cl, Br, I) due to their low ionization energy, react exclusively via charge transfer with NO⁺. Only with C₆H₅F, a small amount of association product (25%) is observed, as the ionization energies are quite similar. However, the investigated benzyl halides C₇H₇X (X = Cl, Br) show halide transfer resulting in a neutral NOX, and only a small percentage of the charge transfer product M⁺ in SIFT-MS (Španěl & Smith, 1999a). [C₆H₅X]⁺ (X = F, Cl, Br, I) is the only observed cation produced by the reaction with O₂⁺. 1-halogenated toluenes, [C₇H₇X]

(X = F, Cl, Br, I) react by charge transfer into M^+ with NO^+ , whereby a small amount of $[M-X]^+$ is observed additionally with O_2^{+*} . This observation flips in the case of benzyl halides C_7H_7X (X = Cl, Br) because the dissociation channel, resulting in $[M-X]^+$, is the main reaction pathway with O_2^{+*} in SIFT-MS (Španěl & Smith, 1999a).



A particularity in the different reaction channels is seen with iodinated compounds, due to the low ionization energy of iodine (IE = 10.45 eV) (Lias et al., 1988) provoking the formation of $[I]^+$ in about 5% for 2-iodotoluene C_7H_7I (Equation 26).

Interestingly, H_3O^+ is an excellent choice as a reagent ion for halogenated aromatic compounds. If the halogen is directly bond to the aromatic ring, only the protonated parent molecule $(MH)^+$ is observed (Španěl & Smith, 1999a). However, monochlorinated and monobrominated ethanes react firstly via hydrogenchlorid and hydrogenbromid elimination, respectively, and secondly via association (Španěl & Smith, 1999a). Association reactions are also observed for chlorinated methyl derivatives. Therefore, only the combination of all three reagent ions H_3O^+ , NO^+ and O_2^{+*} is sufficient for an overall verification of halogenated compounds.

3 | CONCLUSION AND OUTLOOK

While the ionization with NO^+ and O_2^{+*} as reagent ions is widely used in SIFT-MS it presently plays only a minor role in the application of the more sensitive PTR+SRI-MS technique. In contrast to H_3O^+ as the reagent ion, the ionization with NO^+ and O_2^{+*} does not depend on the proton affinity, which extends the number of detectable compounds enormously, as known from their use in SIFT-MS.

The positive charge of the analyte is no longer generated via proton transfer, but by either one of three other reaction pathways, namely hydride abstraction, association reaction or charge transfer reaction. Hydride abstraction, which depends on the hydride affinity of a certain compound compared to the reagent ion takes place exclusively with NO^+ and leads to the development of HNO . The formation of the association product, $[MNO]^+$, proceeds via a three-body association reaction, and is favored if the analyte molecule exhibits a similar ionization energy to NO^+ . Thereby, the phenomenon of charge transfer complexing, in which the positive charge is delocalized over the whole adduct, plays a decisive role. Last but not least, a successful charge transfer reaction, either dissociative or non-dissociative, results

when an analyte's ionization energy is lower than NO^+ or O_2 . Whereas NO^+ is softer, ionization with O_2^{+*} is harsher, making it comparable to electron ionization, and in some cases resulting in signature fragmentation patterns. There are indeed other, more exotic ionization pathways, like hydroxide or sulfhydryl abstraction with NO^+ , but these reactions only play minor roles, as they are observed only for certain classes of substances.

Unfortunately, there is still a lack of knowledge concerning NO^+ and O_2^{+*} ionization in PTR+SRI-MS compared to SIFT-MS, which will hopefully be filled in the near future. Nevertheless, the results given by SIFT-MS can be seen as basis for future research in the field of PTR+SRI-MS. Using each of H_3O^+ and NO^+ as reagent ions, can provide analytical data for many volatile organic compounds, whereas O_2^{+*} is only useful in certain cases. As every reagent ion creates an individual mass spectra of the same complex gas matrix, it is therefore necessary to combine all three specific analysis to obtain a nearly complete analytical determination. This feature, in combination with its high sensitivity, makes PTR+SRI-MS, a leader in qualitative and semi-quantitative analysis.

LIST OF ACRONYMS

CI-MS	chemical Ionization mass spectrometry
EI-MS	electron ionization mass spectrometry
E/N	reduced electric field strength
PTR-MS	proton transfer reaction mass spectrometry
PTR+SRI-MS	proton transfer reaction mass spectrometry with switchable reagent ion capability
SIFDFT-MS	selected ion flow-drift tube mass spectrometry
SIFT-MS	selected ion flow tube mass spectrometry
VOC	volatile organic compound

ACKNOWLEDGMENTS

The authors would like to thank the Max Planck Society for financial support as well as the Federal Ministry of Education and Research (In German: BMBF— Bundesministerium für Bildung und Forschung) for funding the project Carbon2Chem (Subproject LO) Grant No. 03EK3037C. Furthermore, we would like to thank Birgit Deckers and Alina Rettke for the illustrations in this review.

ORCID

Jorge I. Salazar Gómez  <https://orcid.org/0000-0002-6274-9530>

Robert Schlögl  <https://orcid.org/0000-0002-5163-1051>

Holger Ruland  <https://orcid.org/0000-0001-5530-1458>

REFERENCES

- Agarwal B, Gonzalez-Mendez R, Lanza M, Sulzer P, Mark TD, Thomas N, Mayhew CA 2014. Sensitivity and selectivity of switchable reagent ion soft chemical ionization mass spectrometry for the detection of picric acid. *J Phys Chem A*. 118(37):8229-8236.
- Amelynck C, Schoon N, Kuppens T, Bultinck P, Arijs E 2005. A selected ion flow tube study of the reactions of H₃O⁺, NO⁺ and O₂⁺ with some oxygenated biogenic volatile organic compounds. *Int J Mass Spectrom*. 247(1-3):1-9.
- Ard SG, Viggiano AA, Shuman NS 2021. Old school techniques with modern capabilities: Kinetics determination of dynamical information such as barriers, multiple entrance channel complexes, product states, spin crossings, and size effects in metallic ion-molecule reactions. *J Phys Chem A*. 125(17):3503-3527.
- Arnold ST, Viggiano AA, Morris RA 1998. Rate constants and product branching fractions for the reactions of H₃O⁺ and NO⁺ with C₂-C₁₂ alkanes. *J Phys Chem A*. 102:8881-8887.
- Atkinson R, Arey J 2003. Atmospheric degradation of volatile organic compounds. *Chem Rev*. 103(12):4605-4638.
- Barlow SE, Van Doren JM, DePuy CH, Bierbaum VM, Dotan I, Ferguson EE, N. G. Adams, Smith D, Rowe BR, Marquette JB, Dupeyrat G, Durup-Ferguson M 1986. Studies of the reaction of O₂⁺ with deuterated methanes. *J Chem Phys*. 85:3851-3859.
- Biasioli F, Gasperi F, Yeretzian C, Märk TD 2011. PTR-MS monitoring of VOCs and BVOCs in food science and technology. *TrAC Trends in Analytical Chemistry*. 30(7):968-977.
- Blake RS, Monks PS, Ellis AM 2009. Proton-transfer reaction mass spectrometry. *Chem Rev*. 109(3):861-896.
- Blake RS, Ouheda SA, Alwedi EF, Monks PS 2017. Exploration of the utility of CF₃⁺ as a reagent for chemical ionisation reaction mass spectrometry. *Int J Mass Spectrom*. 421:224-233.
- Blake RS, Whyte C, Hughes CO, Ellis AM, Monks PS 2004. Demonstration of proton-transfer reaction time-of-flight mass spectrometry for real-time analysis of trace volatile organic compounds. *Anal Chem* 76(13):3841-3845.
- Blake RS, Wyche KP, Ellis AM, Monks PS 2006. Chemical ionization reaction time-of-flight mass spectrometry: Multi-reagent analysis for determination of trace gas composition. *Int J Mass Spectrom*. 254(1-2):85-93.
- Buhr K, van Ruth S, Delahunty C 2002. Analysis of volatile flavour compounds by proton transfer reaction-mass spectrometry: Fragmentation patterns and discrimination between isobaric and isomeric compounds. *Int J Mass Spectrom*. 221(1):1-7.
- Cappellin L, Makhoul S, Schuhfried E, Romano A, Sanchez del Pulgar J, Aprea E, Farneti B, Costa F, Gasperi F, Biasioli F 2014. Ethylene: Absolute real-time high-sensitivity detection with PTR/SRI-MS. The example of fruits, leaves and bacteria. *Int J Mass Spectrom*. 365-366:33-41.
- Chai J, Miller DJ, Scheuer E, Dibb J, Selimovic V, Yokelson R, Zarzana KJ, Brown SS, Koss AR, Warneke C, Hastings M 2019. Isotopic characterization of nitrogen oxides (NO_x), nitrous acid (HONO), and nitrate (pNO₃⁻) from laboratory biomass burning during FIREX. *Atmos Meas Tech*. 12(12):6303-6317.
- D. Smith PŠ 1996. Ions in the terrestrial atmosphere and in interstellar clouds. *Mass Spectrom Rev*. 14:255-278.
- de Gouw J, Warneke C 2007. Measurements of volatile organic compounds in the earth's atmosphere using proton-transfer-reaction mass spectrometry. *Mass Spectrom Rev*. 26(2):223-257.
- de Gouw JA, Goldan PD, Warneke C, Kuster WC, Roberts JM, Marchewka M, Bertman SB, Pszenny AAP, Keene WC 2003. Validation of proton transfer reaction-mass spectrometry (PTR-MS) measurements of gas-phase organic compounds in the atmosphere during the New England Air Quality Study (NEAQS) in 2002. *J Geophys Res*. 108(D21).
- de Gouw JA, Warneke C, Parrish DD, Holloway JS, Trainer M, Fehsenfeld FC 2003. Emission sources and ocean uptake of acetonitrile (CH₃CN) in the atmosphere. *J Geophys Res*. 108(D11).
- Diskin AM, Wang T, Smith D, Španěl P 2002. A selected ion flow tube (SIFT), study of the reactions of H₃O⁺, NO⁺ and O-2(+) ions with a series of alkenes; in support of SIFT-MS. *Int J Mass Spectrom*. 218(1):87-101.
- Dryahina K, Polášek M, Španěl P 2004. A selected ion flow tube, SIFT, study of the ion chemistry of H₃O⁺, NO⁺ and O₂⁺ ions with several nitroalkanes in the presence of water vapour. *Int J Mass Spectrom*. 239(1):57-65.
- Dunne E, Galbally IE, Lawson S, Patti A 2012. Interference in the PTR-MS measurement of acetonitrile at m/z 42 in polluted urban air—A study using switchable reagent ion PTR-MS. *Int J Mass Spectrom*. 319-320:40-47.
- Durup-Ferguson M, Böhringer H, Fahey DW, Fehsenfeld FC, Ferguson EE 1984. Competitive reaction and quenching of vibrationally excited O+2 ions with SO₂, CH₄, and H₂O. *J Chem Phys*. 81(6):2657-2666.
- Edtbauer A, Hartungen E, Jordan A, Hanel G, Herbig J, Jürschik S, Lanza M, Breiev K, Märk L, Sulzer P 2014. Theory and practical examples of the quantification of CH₄, CO, O₂, and CO₂ with an advanced proton-transfer-reaction/selective-reagent-ionization instrument (PTR/SRI-MS). *Int J Mass Spectrom*. 365-366:10-14.
- Ellis AM, Mayhew CA. *Proton Transfer Reaction Mass Spectrometry. Principles and Applications*. Chichester: Wiley; 2014.
- Erickson MH, Gueneron M, Jobson BT 2014. Measuring long chain alkanes in diesel engine exhaust by thermal desorption PTR-MS. *Atmos Meas Tech*. 7(1):225-239.
- Fabris A, Biasioli F, Granitto PM, Aprea E, Cappellin L, Schuhfried E, Soukoulis C, Mark TD, Gasperi F, Endrizzi I 2010. PTR-TOF-MS and data-mining methods for rapid characterisation of agro-industrial samples: Influence of milk storage conditions on the volatile compounds profile of Trentingrana cheese. *J Mass Spectrom*. 45(9):1065-1074.
- Fehsenfeld FC, Schmeltekopf AL, Goldan PD, Schiff HI, Ferguson EE 1966. Thermal energy ion—neutral reaction rates. I. Some reactions of helium ions. *J Chem Phys* 44(11):4087-4094.
- Gallardo-Escamilla FJ, Kelly AL, Delahunty CM 2005. Sensory characteristics and related volatile flavor compound profiles of different types of whey. *J Dairy Sci*. 88(8):2689-2699.
- Gochel-Dupuis M, Delwiche J, Hubin-Franskin M-J, Collin JE 1992. High-resolution HeI photoelectron spectrum of acetonitrile. *Chem Phys Lett*. 193:41-48.
- Graus M, Müller M, Hansel A 2010. High resolution PTR-TOF: Quantification and formula confirmation of VOC in real time. *J Am Soc Mass Spectrom*. 21(6):1037-1044.

- Haick H, Broza YY, Mochalski P, Ruzsanyi V, Amann A 2014. Assessment, origin, and implementation of breath volatile cancer markers. *Chem Soc Rev*. 43(5):1423-1449.
- Hansel A, Jordan A, Holzinger R, Prazeller P, Vogel W, Lindinger W 1995. Proton transfer reaction mass spectrometry: On-line trace gas analysis at the ppb level. *Int J Mass Spectrom Ion Process* 609-619.
- Hastie C, Thompson A, Perkins M, Langford VS, Eddleston M, Homer NZM 2021. Selected ion flow tube-mass spectrometry (SIFT-MS) as an alternative to gas chromatography/mass spectrometry (GC/MS) for the analysis of cyclohexanone and cyclohexanol in plasma. *ACS Omega*.
- Haynes WM, Lide DR, Bruno TJ. 2016–2017. *CRC Handbook of Chemistry and Physics: A Ready-reference Book of Chemical and Physical Data*. 97th ed. Boca Raton, FL: CRC Press.
- Hayward S, Hewitt CN, Sartin JH, Owen SM 2002. Performance characteristics and applications of a proton transfer reaction-mass spectrometer for measuring volatile organic compounds in ambient air. *Environ Sci Technol*. 36(7):1554-1560.
- Hearn JD, Smith GD 2004. A chemical ionization mass spectrometry method for the online analysis of organic aerosols. *Anal Chem*. 76(10):2820-2826.
- Hera D, Langford V, McEwan M, McKellar T, Milligan D 2017. Negative reagent ions for real time detection using SIFT-MS. *Environments*. 4(1).
- Herbig J, Muller M, Schallhart S, Titzmann T, Graus M, Hansel A 2009. On-line breath analysis with PTR-TOF. *J Breath Res*. 3(2):027004.
- Hlastala MP 1998. The alcohol breath test—A review. *J Appl Physiol* 84:401-408.
- Holleman AF, Wiberg E, Wiberg N. *Lehrbuch der anorganischen Chemie*. 102nd ed. Berlin: Walter de Gruyter & Co.; 2007.
- Hunt DF, Harvey TM 1975. Nitric oxide chemical ionization mass spectra of alkanes. *Anal Chem*. 47(12):1965-1969.
- Hunt DF, Harvey TM 1975. Nitric oxide chemical ionization mass spectra of olefins. *Anal Chem*. 47(13):2136-2141.
- Hunt DF, Harvey TM, Brumley WC, Ryan III JF, Russel JW 1982. Nitric oxide chemical ionization mass spectrometry of alcohols. *Anal Chem*. 54(3):492-496.
- Hunt DF, Ryan JF 1972. Chemical ionization mass spectrometry studies. Nitric oxide as a reagent gas. *J Chem Soc Chem Commun*. (10):620-621.
- Hunter E, Lias S 1998. Evaluated gas phase basicities and proton affinities of molecules: An update. *J Phys Chem Ref Data* 27: 413-656.
- IONICON. *User Manual PTR-MS 2019: Hands-on*. Innsbruck: IO-NICON Analytik GmbH; 2019.
- Jarvis GK, Kennedy RA, Mayhew CA, Tuckett RP 2000. Charge transfer from neutral perfluorocarbons to various cations: Long-range versus short-range reaction mechanisms. *Int J Mass Spectrom*. 202(1-3):323-343.
- Jobson BT, Alexander ML, Maupin GD, Muntean GG 2005. On-line analysis of organic compounds in diesel exhaust using a proton transfer reaction mass spectrometer (PTR-MS). *Int J Mass Spectrom*. 245(1-3):78-89.
- Jordan A, Haidacher S, Hanel G, Hartungen E, Herbig J, Märk L, Schottkowsky R, Seehauser H, Sulzer P, Märk TD 2009a. An online ultra-high sensitivity proton-transfer-reaction mass-spectrometer combined with switchable reagent ion capability (PTR+SRI-MS). *Int J Mass Spectrom*. 286(1):32-38.
- Jordan A, Haidacher S, Hanel G, Hartungen E, Märk L, Seehauser H, Schottkowsky R, Sulzer P, Märk TD 2009b. A high resolution and high sensitivity proton-transfer-reaction time-of-flight mass spectrometer (PTR-TOF-MS). *Int J Mass Spectrom*. 286(2-3):122-128.
- Jurschik S, Agarwal B, Kassebacher T, Sulzer P, Mayhew CA, Mark TD 2012. Rapid and facile detection of four date rape drugs in different beverages utilizing proton transfer reaction mass spectrometry (PTR-MS). *J Mass Spectrom*. 47(9): 1092-1097.
- Jürschik S, Sulzer P, Petersson F, Mayhew CA, Jordan A, Agarwal B, Haidacher S, Seehauser H, Becker K, Märk TD 2010. Proton transfer reaction mass spectrometry for the sensitive and rapid real-time detection of solid high explosives in air and water. *Anal Bioanal Chem*. 398(7-8):2813-2820.
- Karl T, Hansel A, Cappellin L, Kaser L, Herdinger-Blatt I, Jud W 2012. Selective measurements of isoprene and 2-methyl-3-buten-2-ol based on NO⁺ ionization mass spectrometry. *Atmos Chem Phys*. 12(24):11877-11884.
- Keck L, Oeh U, Hoeschen C 2007. Corrected equation for the concentrations in the drift tube of a proton transfer reaction-mass spectrometer (PTR-MS). *Int J Mass Spectrom*. 264(1):92-95.
- Klapstein D, MacPherson CD, O'Brien RT 1990. The photoelectron spectra and electronic structure of 2-carbonyl furans. *Can J Chem*. 68(5):747-754.
- Knighton WB, Fortner EC, Midey AJ, Viggiano AA, Herndon SC, Wood EC, Kolb CE 2009. HCN detection with a proton transfer reaction mass spectrometer. *Int J Mass Spectrom*. 283(1-3):112-121.
- Knighton WB, Herndon SC, Franklin JF, Wood EC, Wormhoudt J, Brooks W, Fortner EC, Allen DT 2012. Direct measurement of volatile organic compound emissions from industrial flares using real-time online techniques: Proton transfer reaction mass spectrometry and tunable infrared laser differential absorption spectroscopy. *Ind Eng Chem Res*. 51(39): 12674-12684.
- Koss AR, Warneke C, Yuan B, Coggon MM, Veres PR, de Gouw JA 2016. Evaluation of NO⁺ reagent ion chemistry for online measurements of atmospheric volatile organic compounds. *Atmos Meas Tech*. 9(7):2909-2925.
- Lehnert A-S, Behrendt T, Ruecker A, Pohnert G, Trumbore SE 2020. SIFT-MS optimization for atmospheric trace gas measurements at varying humidity. *AtmMeas Tech*. 13(7): 3507-3520.
- Li R, Warneke C, Graus M, Field R, Geiger F, Veres PR, Soltis J, Li SM, Murphy SM, Sweeney C, Pétron G, Roberts JM, de Gouw J 2014. Measurements of hydrogen sulfide (H₂S) using PTR-MS: Calibration, humidity dependence, inter-comparison and results from field studies in an oil and gas production region. *Atmos Meas Tech*. 7(10):3597-3610.
- Lias SG, Bartmess JE, Liebman JF, Holmes JL, Levin RD, Mallard WG 1988. *J Phys Chem Ref Data, Suppl* 17:1-867.
- Lindinger C, Pollen P, Ali S, Yeretizian C, Blank I, Märk T 2005. Unambiguous identification of volatile organic compounds by proton-transfer reaction mass spectrometry coupled with GC/MS. *Anal Chem*. 77:4117 - 4124.
- Lindinger W, Hansel A, Jordan A 1998. On-line monitoring of volatile organic compounds at pptv levels by means of proton-transfer-reaction mass spectrometry (PTR-MS) medical

- applications, food control and environmental research. *Int J Mass Spectrom Ion Processes* 173(3):191-241.
- Lirk P, Bodrogi F, Deibl M, Kähler CM, Colvin J, Moser B, Pinggera G, Raifer H, Rieder J, Schobersberger W 2004. Quantification of recent smoking behaviour using proton transfer reaction-mass spectrometry (PTR-MS). *Wien Klin Wochenschr* 1161-2:21-25.
- Liu YJ, Herdinger-Blatt I, McKinney KA, Martin ST 2013. Production of methyl vinyl ketone and methacrolein via the hydroperoxyl pathway of isoprene oxidation. *Atmos Chem Phys* 13(11):5715-5730.
- M. Coelho Neto D, L. P. Ferreira L, M. S. Sad C, S. Borges W, V. R. Castro E, R. Filgueiras P, Lacerda Jr. V 2020. Chemical concepts involved in beer production: A review. *Revista Virtual de Química* 12(1):120-147.
- Maleknia SD, Bell TL, Adams MA 2007. PTR-MS analysis of reference and plant-emitted volatile organic compounds. *Int J Mass Spectrom* 262(3):203-210.
- Mielke LH, Erickson DE, McLuckey SA, Muller M, Wisthaler A, Hansel A, Shepson PB 2008. Development of a proton-transfer reaction-linear ion trap mass spectrometer for quantitative determination of volatile organic compounds. *Anal Chem* 80(21):8171-8177.
- Misztal PK, Heal MR, Nemitz E, Cape JN 2012. Development of PTR-MS selectivity for structural isomers: Monoterpenes as a case study. *Int J Mass Spectrom* 310:10-19.
- Mochalski P, Unterkofler K, Spanel P, Smith D, Amann A 2014a. Product ion distributions for the reactions of NO(+) with some physiologically significant aldehydes obtained using a SRI-TOF-MS instrument. *Int J Mass Spectrom* 363:23-31.
- Mochalski P, Unterkofler K, Spanel P, Smith D, Amann A 2014b. Product ion distributions for the reactions of NO(+) with some physiologically significant volatile organosulfur and organoselenium compounds obtained using a selective reagent ionization time-of-flight mass spectrometer. *Rapid Commun Mass Spectrom* 28(15):1683-1690.
- Mochalski P, Unterkofler K, Španěl P, Smith D, Amann A 2015. Product ion distributions for the reactions of NO⁺ with some N-containing and O-containing heterocyclic compounds obtained using SRI-TOF-MS. *Int J Mass Spectrom* 386:42-46.
- Moussa SG, Leithead A, Li S-M, Chan TW, Wentzell JJB, Stroud C, Zhang J, Lee P, Lu G, Brook JR, Hayden K, Narayan J, Liggio J 2016. Emissions of hydrogen cyanide from on-road gasoline and diesel vehicles. *Atmos Environ* 131:185-195.
- Myhre G, Shindell D, Bréon F-M, Collins W, Fuglestedt J, Huang J, Koch D, Lamarque J-F, Lee D, Mendoza B, Nakajima T, Robock A, Stephens G, Takemura T, Zhang H. Anthropogenic and Natural Radiative Forcing Supplementary Material. In: Climate Change 2013: The Physical Science Basis. Contribution of Working Group I to the Fifth Assessment Report of the Intergovernmental Panel on Climate Change. Available from www.climatechange2013.org and www.ipcc.ch; 2013.
- N. G. Adams, Smith D 1976. The selected ion flow tube (SIFT); a technique for studying ion-neutral reactions. *Int J Mass Spectrom Ion Physics* 21:349.
- Nemeth GI, Selzle HL, Schlag EW 1993. Magnetic ZEKE experiments with mass analysis. *Chem Phys Lett* 215(1-3): 151-155.
- Norman M, Hansel A, Wisthaler A 2007. O₂⁺ as reagent ion in the PTR-MS instrument: Detection of gas-phase ammonia. *Int J Mass Spectrom* 265(2-3):382-387.
- Ohno K, Okamura K, Yamakado H, Hoshino S, Takami T, Yamauchi M 1995. Penning Ionization of HCHO, CH₂CH₂, and CH₂CHCHO by collision with He*(23S) metastable atoms. *J Chem Phys* 99:14247-14253.
- Pagonis D, Sekimoto K, de Gouw J 2019. A library of proton-transfer reactions of H₃O⁺ ions used for trace gas detection. *J Am Soc Mass Spectrom* 30(7):1330-1335.
- Prazeller P, Palmer PT, Boscaini E, Jobson T, Alexander M 2003. Proton transfer reaction ion trap mass spectrometer. *Rapid Commun Mass Spectrom* 17(14):1593-1599.
- Pugliese G, Trefz P, Brock B, Schubert JK, Miekisch W 2019. Extending PTR based breath analysis to real-time monitoring of reactive volatile organic compounds. *Analyst* 144(24): 7359-7367.
- Pysanenko A, Spanel P, Smith D 2008. A study of sulfur-containing compounds in mouth- and nose-exhaled breath and in the oral cavity using selected ion flow tube mass spectrometry. *J Breath Res* 2(4):046004.
- Romano A, Hanna GB 2018. Identification and quantification of VOCs by proton transfer reaction time of flight mass spectrometry: An experimental workflow for the optimization of specificity, sensitivity, and accuracy. *J Mass Spectrom* 53(4):287-295.
- Sanchez del Pulgar J, Soukoulis C, Carrapiso AI, Cappellin L, Granitto P, Aprea E, Romano A, Gasperi F, Biasioli F 2013. Effect of the pig rearing system on the final volatile profile of Iberian dry-cured ham as detected by PTR-ToF-MS. *Meat Sci* 93(3):420-428.
- Schittkowski J, Ruland H, Laudenschleger D, Girod K, Kähler K, Kaluza S, Muhler M, Schlögl R 2018. Methanol synthesis from steel mill exhaust gases: Challenges for the industrial Cu/ZnO/Al₂O₃ catalyst. *Chem Ing Tech* 90(10): 1419-1429.
- Schoon N, Amelynck C, Debie E, Bultinck P, Arijs E 2007. A selected ion flow tube study of the reactions of H₃O⁺, NO⁺ and O₂⁺ with a series of C₅, C₆ and C₈ unsaturated biogenic alcohols. *Int J Mass Spectrom* 263(2-3):127-136.
- Smith D, Adams NG 1987. *Adv Atom Mol Phys* 24:1-49.
- Smith D, Cheng P, Španěl P 2002. Analysis of petrol and diesel vapour and vehicle engine exhaust gases using selected ion flow tube mass spectrometry. *Rapid Commun Mass Spectrom* 16(11):1124-1134.
- Smith D, Chippendale TW, Španěl P 2014. Reactions of the selected ion flow tube mass spectrometry reagent ions H₃O⁺ and NO⁺ with a series of volatile aldehydes of biogenic significance. *Rapid Commun Mass Spectrom* 28(17):1917-1928.
- Smith D, Diskin AM, Ji Y, Španěl P 2001. Concurrent use of H₃O⁺, NO⁺, and O₂⁺ precursor ions for the detection and quantification of diverse trace gases in the presence of air and breath by selected ion-flow tube mass spectrometry. *Int J Mass Spectrom* 209:81-97.

- Smith D, Španěl P 1996. The novel selected-ion flow tube approach to trace gas analysis of air and breath. *Rapid Commun Mass Spectrom.* 1183-1198.
- Smith D, Španěl P 2005. Selected ion flow tube mass spectrometry (SIFT-MS) for on-line trace gas analysis. *Mass Spectrom Rev.* 24(5):661-700.
- Smith D, Španěl P 2011. Direct, rapid quantitative analyses of BVOCs using SIFT-MS and PTR-MS obviating sample collection. *TrAC Trends in Analytical Chemistry.* 30(7):945-959.
- Smith D, Španěl P, Dryahina K 2019. H₃O⁺, NO⁺ and O₂⁺ reactions with saturated and unsaturated monoketones and diones; focus on hydration of product ions. *Int J Mass Spec.* 435:173-180.
- Smith D, Španěl P, Herbig J, Beauchamp J 2014. Mass spectrometry for real-time quantitative breath analysis. *J Breath Res.* 8(2): 027101.
- Smith D, Španěl P, Holland TA, Al Singari W, Elder JB 1999. Analysis of formaldehyde in the headspace of urine from bladder and prostate cancer patients using selected ion flow tube mass spectrometry. *Rapid Commun Mass Spectrom* 13(14):724-729.
- Smith D, Španěl P, Thompson JM, Cocker J, Rolfe P 1998. *Appl Occup Environ Hygiene* 13:817-825.
- Sovova K, Shestivska V, Španěl P 2012. Real-time quantification of traces of biogenic volatile selenium compounds in humid air by selected ion flow tube mass spectrometry. *Anal Chem.* 84(11):4979-4983.
- Španěl P, Li Y, Smith D 1997. SIFT studies of the reactions of H₃O⁺, NO⁺ and O₂⁺ with a series of aldehydes and ketones. *Int J Mass Spectrom Ion Process* 165/166:25-37.
- Španěl P, Smith D 1996a. A selected ion flow tube study of the reactions of NO⁺ and O₂⁺ ions with some organic molecules: The potential for trace gas analysis of air. *J Chem Phys.* 104(5): 1893-1899.
- Španěl P, Smith D 1996b. Selected ion flow tube: A technique for quantitative trace gas analysis of air and breath. *Med & Biol Eng Comput* 34(6):409-419.
- Španěl P, Smith D 1997. SIFT studies of the reactions of H₃O⁺, NO⁺ and O₂⁺ with a series of alcohols. *Int J Mass Spectrom Ion Process.* 167/168:375-388.
- Španěl P, Smith D 1998a. Selected ion flow tube studies of the reactions of H₃O⁺, NO⁺ and O₂⁺ with several amines and some other nitrogen-containing molecules. *Int J Mass Spectrom* 176:203-211.
- Španěl P, Smith D 1998b. Selected ion flow tube studies of the reactions of H₃O⁺, NO⁺ and O₂⁺ with several aromatic and aliphatic hydrocarbons. *Int J Mass Spectrom* 181:1-10.
- Španěl P, Smith D 1998c. Selected ion flow tube studies of the reactions of H₃O⁺, NO⁺ and O₂⁺ with some organosulphur molecules. *Int J Mass Spectrom.* 176:167-176.
- Španěl P, Smith D 1998d. SIFT studies of the reactions of H₃O⁺, NO⁺ and O₂⁺ with a series of volatile carboxylic acids and esters. *Int J Mass Spectrom Ion Process* 172: 137-147.
- Španěl P, Smith D 1998e. SIFT studies of the reactions of H₃O⁺, NO⁺ and O₂⁺ with several ethers. *Int J Mass Spectrom Ion Process* 172:239-247.
- Španěl P, Smith D 1999a. Selected ion flow tube studies of the reactions of H₃O⁺, NO⁺ and O₂⁺ with several aromatic and aliphatic monosubstituted halocarbons. *Int J Mass Spectrom.* 189:213-223.
- Španěl P, Smith D 1999b. Selected ion flow tube studies of the reactions of H₃O⁺, NO⁺ and O₂⁺ with some chloroalkanes and chloroalkenes. *Int J Mass Spectrom.* 184:175-181.
- Španěl P, Smith D 1999c. Selected ion flow tube studies of the reactions of H₃O⁺, NO⁺ and O₂⁺ with eleven amine structural isomers of C₅H₁₃N. *Int J Mass Spectrom* 185/186/ 187:139-147.
- Španěl P, Zabka J, Zymak I, Smith D 2017. Selected ion flow tube study of the reactions of H₃O⁺ and NO⁺ with a series of primary alcohols in the presence of water vapour in support of selected ion flow tube mass spectrometry. *Rapid Commun Mass Spectrom.* 31(5):437-446.
- Spesvyi A, Smith D, Španěl P 2017. Ion chemistry at elevated ion-molecule interaction energies in a selected ion flow-drift tube: Reactions of H₃O⁺, NO⁺ and O₂⁺ with saturated aliphatic ketones. *Phys Chem Chem Phys.* 19(47): 31714-31723.
- Spesvyi A, Sovová K, Španěl P 2016. In-tube collision-induced dissociation for selected ion flow-drift tube mass spectrometry, SIFDT-MS: A case study of NO⁺ reactions with isomeric monoterpenes. *Rapid Commun Mass Spectrom.* 30(18): 2009-2016.
- Strekowski RS, Alvarez C, Petrov-Stojanović J, Hagebaum-Reignier D, Wortham H 2019. Theoretical chemical ionization rate constants of the concurrent reactions of hydronium ions (H₃O⁺) and oxygen ions (O₂⁺) with selected organic iodides. *J Mass Spectrom.* 54(5):422-428.
- Sulzer P, Agarwal B, Jürschik S, Lanza M, Jordan A, Hartungen E, Hanel G, Märk L, Märk TD, González-Méndez R, Watts P, Mayhew CA 2013. Applications of switching reagent ions in proton transfer reaction mass spectrometric instruments for the improved selectivity of explosive compounds. *Int J Mass Spectrom.* 354-355:123-128.
- Sulzer P, Edtbauer A, Hartungen E, Jürschik S, Jordan A, Hanel G, Feil S, Jaksch S, Märk L, Märk TD 2012. From conventional proton-transfer-reaction mass spectrometry (PTR-MS) to universal trace gas analysis. *Int J Mass Spectrom.* 321-322:66-70.
- Sulzer P, Hartungen E, Hanel G, Feil S, Winkler K, Mutschlechner P, Haidacher S, Schottkowsky R, Gansch D, Seehauser H, Striednig M, Jürschik S, Breiev K, Lanza M, Herbig J, Märk L, Märk TD, Jordan A 2014. A proton transfer reaction-quadrupole interface time-of-flight mass spectrometer (PTR-QiTOF): High speed due to extreme sensitivity. *Int J Mass Spectrom.* 368:1-5.
- Van Doren JM, Barlow SE, DePuy CH, Bierbaum VM, Dotan I 1986. Chemistry and Structure of the CH₃O₂⁺ Product of the O₂⁺ + CH₄ Reaction. *J Chem Phys.* 90:2772-2777.
- Veres P, Roberts JM, Warneke C, Welsh-Bon D, Zahniser M, Herndon S, Fall R, de Gouw J 2008. Development of negative-ion proton-transfer chemical-ionization mass spectrometry (NI-PT-CIMS) for the measurement of gas-phase organic acids in the atmosphere. *Int J Mass Spectrom.* 274(1-3):48-55.

- Walters EA, Blais NC 1984. Structure and binding energy of the H₂S dimer at the CCSD(T) complete basis set limit. *J Chem Phys.* 80(7):4208-4213.
- Wang T, Španěl P, Smith D 2004. A selected ion flow tube study of the reactions of H₃O⁺, NO⁺ and O₂⁺ with some phenols, phenyl alcohols and cyclic carbonyl compounds in support of SIFT-MS and PTR-MS. *Int J Mass Spectrom.* 239(2-3):139-146.
- Warneke C, Gouw JA, Lovejoy ER, Murphy PC, Kuster WC, Fall R 2005. Development of proton-transfer ion trap-mass spectrometry: On-line detection and identification of volatile organic compounds in air. *J Am Soc Mass Spectrom.* 16(8):1316-1324.
- Warneke C, Veres P, Holloway JS, Stutz J, Tsai C, Alvarez S, Rappenglueck B, Fehsenfeld FC, Graus M, Gilman JB, de Gouw JA 2011. Airborne formaldehyde measurements using PTR-MS: Calibration, humidity dependence, inter-comparison and initial results. *Atmos Meas Tech.* 4(10):2345-2358.
- Wedlan F, Atkinson DB 2003. Membrane introduction mass spectrometry of nonpolar hydrocarbons using nitric oxide chemical ionization. *Environ Sci Technol.* 37(19):4425-4428.
- White IR, Willis KA, Whyte C, Cordell R, Blake RS, Wardlaw AJ, Rao S, Grigg J, Ellis AM, Monks PS 2013. Real-time multi-marker measurement of organic compounds in human breath: Towards fingerprinting breath. *J Breath Res.* 7(1):017112.
- Williams BA, Cool TA 1991. Two-photon spectroscopy of Rydberg states of jet-cooled C₂H₄ and C₂D₄. *J Chem Phys.* 94:6358-6366.
- Williamson AD, Beauchamp JL 1974. Ion-molecule reactions of NO⁺ with organic molecules by ion cyclotron resonance spectroscopy. *J Am Chem Soc* 97:5714-5718.
- Wilson PF, Freeman CG, McEwan MJ 2003. Reactions of small hydrocarbons with H₃O⁺, O₂⁺ and NO⁺ ions. *Int J Mass Spectrom.* 229(3):143-149.
- Wyche KP, Blake RS, Willis KA, Monks PS, Ellis AM 2005. Differentiation of isobaric compounds using chemical ionization reaction mass spectrometry. *Rapid Commun Mass Spectrom.* 19(22):3356-3362.
- Yeretzian C, Jordan A, Lindinger W 2003. Analysing the headspace of a coffee by proton-transfer-reaction mass spectrometry. *Int J Mass Spectrom.* 223-224:115-139.
- Yuan B, Koss A, Warneke C, Gilman JB, Lerner BM, Stark H, de Gouw JA 2016. A high-resolution time-of-flight chemical ionization mass spectrometer utilizing hydronium ions (H₃O⁺-ToF-CIMS) for measurements of volatile organic compounds in the atmosphere. *Atmos Meas Tech.* 9(6):2735-2752.
- Yuan B, Koss AR, Warneke C, Coggon M, Sekimoto K, de Gouw JA 2017. Proton-transfer-reaction mass spectrometry: Applications in atmospheric sciences. *Chem Rev.* 117(21):13187-13229.
- Yuan B, Warneke C, Shao M, de Gouw JA 2014. Interpretation of volatile organic compound measurements by proton-transfer-reaction mass spectrometry over the deepwater horizon oil spill. *Int J Mass Spectrom.* 358:43-48.
- Zhao J, Zhang R 2004. Proton transfer reaction rate constants between hydronium ion (H₃O⁺) and volatile organic compounds. *Atmos Environ.* 38(14):2177-2185.

- Zhao J, Zhang RY, Fortner EC, North SW 2004. Quantification of hydroxycarbonyls from OH-isoprene reactions. *J Am Chem Soc.* 126(9):2686-2687.

AUTHOR BIOGRAPHIES



Oliver Hegen, born in 1987 in Neuburg a. d. Donau, Germany, received his PhD at the University of Regensburg in 2018, where he focussed on the synthesis of inorganic polymers at the working group of M. Scheer. In 2019, he switched his focus towards analytical chemistry at the Max Planck Institute for Chemical Energy conversion in the working group of H. Ruland at the project Carbon2Chem®. Thereby, he is especially interested in quantitative and qualitative analysis of traces in exhaust gas with proton-transfer-reaction mass spectrometry (PTR-MS) and gas chromatography.



Jorge Iván Salazar Gómez, born in 1977 in Medellín, Colombia, received his PhD at the University of Strathclyde in Glasgow, UK in 2006. In 2007, he changed his perspective towards environmental topics, working on the catalytic purification of landfill gases, the characterization of biogases and on the development of thermochemical storage materials at the Fraunhofer Institute for Environmental, Safety, and Energy Technology UM-SICHT. In 2014, he moved to the Max Planck Institute for Chemical Energy Conversion working in the project HüGaProp and currently in the Carbon2Chem® project. His present research interest focuses on the characterization of traces in complex gas matrices with Proton-Transfer-Reaction Mass Spectrometry (PTR-MS).



Robert Schlögl studied in Munich and habilitated with Prof. Ertl in Berlin. Since 1994, he has been director at the Fritz Haber Institute of the Max Planck Society (Berlin) and, in addition, since 2011, founding director of the Max Planck Institute for Chemical Energy Conversion (Mülheim a.d. Ruhr). He is a member of the Leopoldina, acatech and the BBAW. His research focuses on inorganic chemistry, heterogeneous catalysis, nanostructures, materials research for chemical energy conversion, and concepts for sustainable energy supply and storage.



Holger Ruland studied chemistry in Bochum and Cologne, Germany. After receiving his PhD in 2011, he coordinated the work on syngas chemistry in the Group of Industrial Chemistry at the Ruhr University Bochum, before he changed to the Max Planck Institute of Chemical Energy Conversion. Since 2018 he is the Head of the Catalytic Technology Group in the Heterogeneous Reactions Department at MPI CEC focusing on catalytic reactions for highly efficient and cost-effective energy conversion and storage

with a special focus on catalytic options for carbon capture and utilization (CCU) from industrial exhaust gases.

How to cite this article: Hegen O, Salazar Gomez IS, Schlögl R, Ruland H. The potential of NO^+ and O_2^{+*} in switchable reagent ion proton transfer reaction time-of-flight mass spectrometry. *Mass Spec Rev.* 2023;42:1688–1726.

<https://doi.org/10.1002/mas.21770>